172
06/30/80 MM

Hi. 1421

LA-8386-PR

Progress Report

General-Purpose Heat Source Project and Space Nuclear Safety and Fuels Program

February 1980

MASTER

University of California

LOS ALAMOS SCIENTIFIC LABORATORY
Post Office Box 1663 Los Alamos, New Mexico 87545

LA-8386-PR
Progress Report
UC-23
Issued: May 1980

General-Purpose Heat Source Project and Space Nuclear Safety and Fuels Program

February 1980

Compiled by
W. J. Maraman

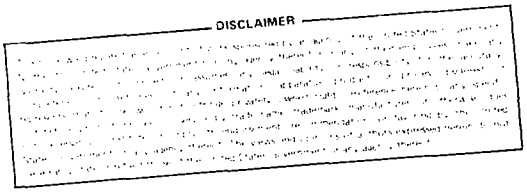

ABSTRACT

This formal monthly report covers the studies related to the use of $^{238}PuO_2$ in radioisotopic power systems carried out for the Advanced Nuclear Systems and Projects Division of the Los Alamos Scientific Laboratory. The two programs involved are the following:

General-Purpose Heat Source Development

Space Nuclear Safety and Fuels.

Most of the studies discussed here are of a continuing nature. Results and conclusions described may change as the work continues. Published reference to the results cited in this report should not be made without the explicit permission of the person in charge of the work.

GENERAL-PURPOSE HEAT SOURCE PROJECT AND
SPACE NUCLEAR SAFETY AND FUELS PROGRAM

FEBRUARY 1980

Compiled by

W. J. Maraman

I. GENERAL-PURPOSE HEAT SOURCE

A. Schedule

The current schedule for the remainder of the General-Purpose Heat Source (GPHS) project is given in Fig. I-1.

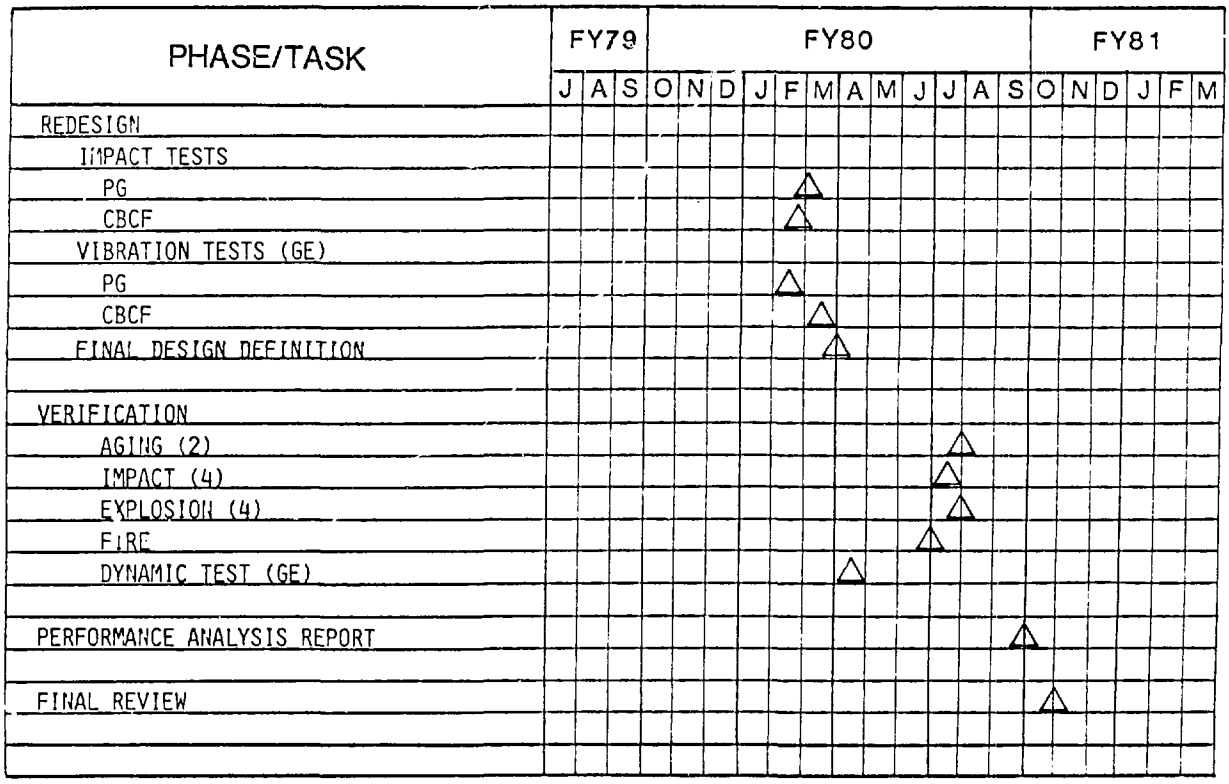

Fig. I-1.
Current GPHS project schedule.

B. Design Impact Tests

One successful impact test was carried out this month and the microstructural analyses of two previously impacted samples were completed.

1. CBCF vs. Pyrolytic Graphite (PG) Insulation. An impact test series of four GPHS modules has been planned to allow direct comparisons of the impact responses of the two current module concepts, one insulated with the low density CBCF insulation and the other insulated with PG. The test conditions were selected by the GPHS prime contractor, General Electric Company (GE), and the Department of Energy (DOE). One module of each insulation design is to be impacted at 0° (along the graphite impact shell (GIS) axis) and another pair is to be impacted at 45° (along the large-face diagonal). The impact temperature for these four tests will be 965°C and the impact velocity will be 58 m/s. The iridium capsules will be heat treated for 20 h at 1500°C to provide a grain size of 12-14/thickness. The aeroshells are to be machined to simulate the ablation that would occur during reentry prior to impact.

a. DAGCI-0-C1. This was a double impact at 0° (end-on). The GIS was of design DGIS-14, as shown in Fig. I-2. The side-wall thickness of 4.24 mm, end-wall thickness of 5.84 mm, and the 16% area fraction hole pattern in the ends are the same as those used in designs DGIS-12 and -13. It also contained a single threaded closure on the impact end and a standard web. The GIS was machined from fine-weave, pierced fabric (FWPF) composite outgassed 1 h at 1800°C. The GIS was surrounded by CBCF insulation provided by Oak Ridge National Laboratory (ORNL) and enclosed in a FWPF composite aeroshell, as shown in Fig. I-3. No GIS-GIS interaction occurs in an 0° impact event, but after the initial crush-up, resistance to further lateral displacement is afforded by the adjacent GIS and the aeroshell wall outermost from the test GIS.

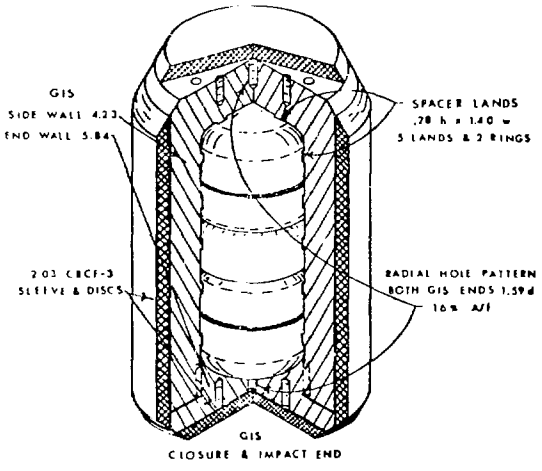

Fig. I-2.
CBCF-insulated impact assembly used in tests DAGCI-0-C1 (0°) and MAGCI-45-110-C1 (45°).

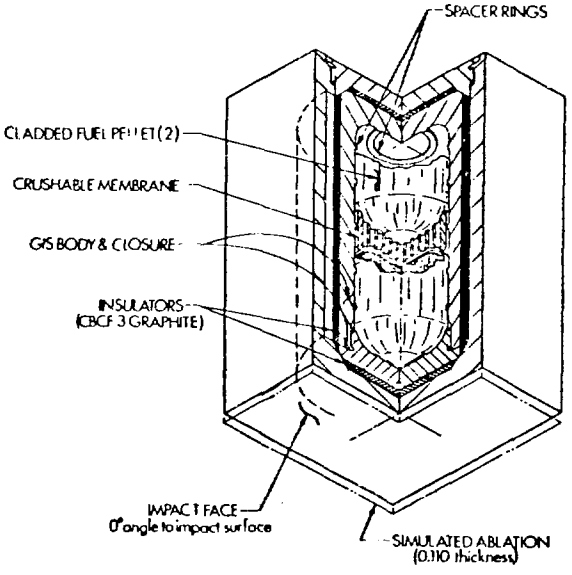

Fig. I-3.
DAGCI-0-C1. Sketch of aeroshell and GIS assembly for this double 0° impact with CBCF insulation.

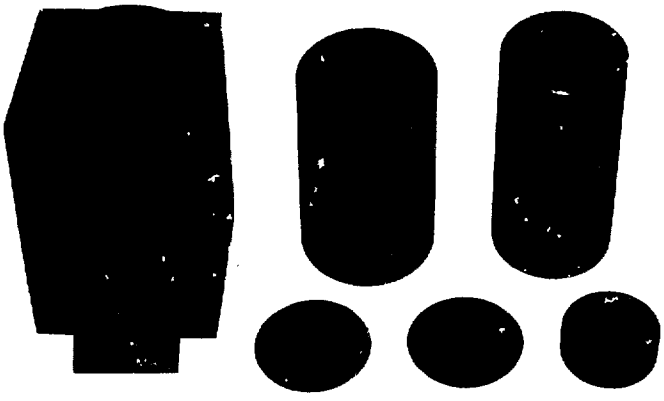

Fig. I-4.
Photograph of DAGCI-O-Cl assembly before impact.

Consequently, to provide a valid approximation to a full module without using a second GIS, a void volume with the correct module "window" dimensions was designed for both LMRC and LMRE 0° impact tests. A 2.9-mm maximum free lateral movement was provided in the 0° impact modules. The leading face of the aeroshell was machined to a thickness of 2.79 mm to simulate ablation. The assembly before impact is shown in Fig. I-4.

The leading capsule was IRG-59, Ir-0.3% W. It was annealed for 20 h at 1500°C before welding and subjected to thermal reentry pulse with the $^{238}PuO_2$ pellet after welding. The maximum temperature of the reentry pulse was 1700°C, with a total of 6 minutes above 1300°C. The temperature profile is similar to that shown in the November 1979 report. The capsule contained a $^{238}PuO_2$ fuel pellet of 84.3% theoretical density. The trailing capsule was GCI-40 containing a UO_2 pellet. The assembly was impacted at 0°, 58.3 m/s, and 965°C.

The impacted aeroshell is shown in Fig. I-5 and the GIS is pictured in Fig. I-6. The front of the aeroshell tore off, whereas the rest of it remained intact. The GIS suffered several fractures as shown in the figures, but also

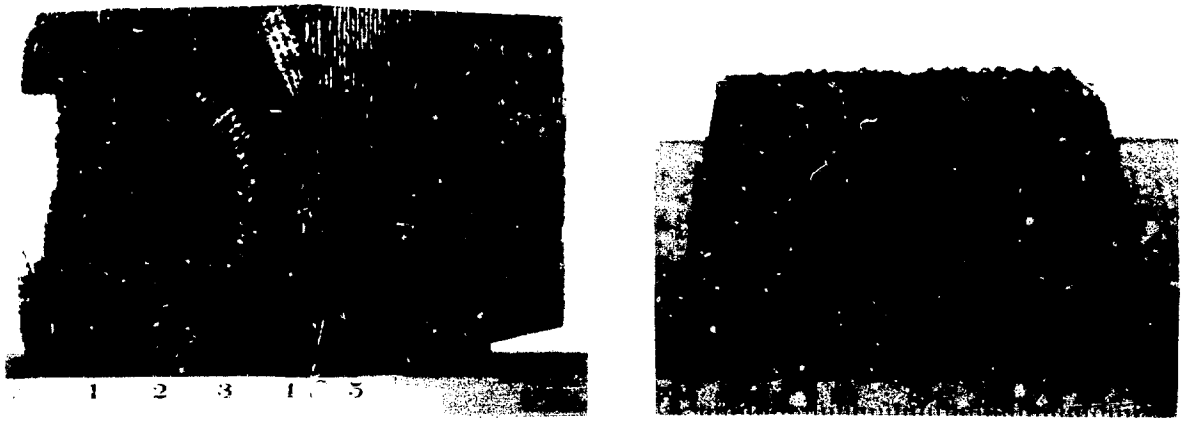

(a) (b)

Fig. I-5.
DAGCI-O-Cl: Double 0° impact with leading capsule IRG-59 in DGIS-14. Impacted at 0°, 58.3 m/s, and 965°C. (a) Shows oblique view of remairs of aeroshell and end of DGIS and (b) shows end cap of aeroshell torn off during impact.

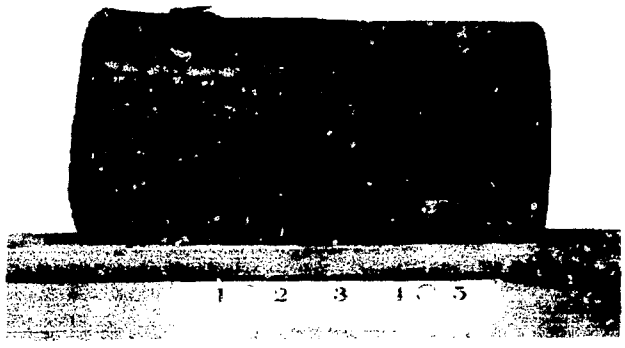

(a)

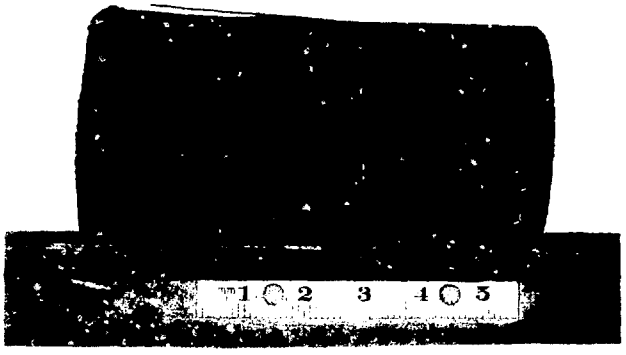

(b)

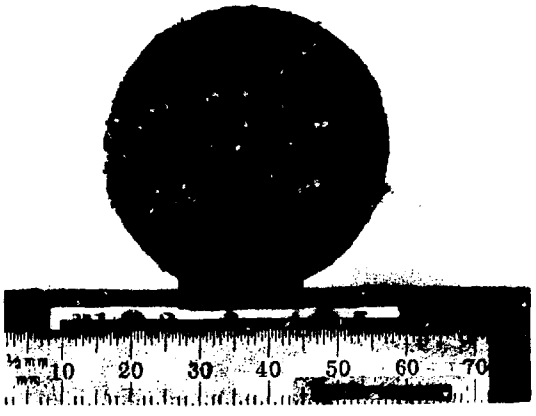

(c)

Fig. I-6.
DAGCI-0-C1: Double GIS of impact shown in Fig. I-4. (a) and (b) show fractures in double GIS at two orientations, (c) shows impact end of double GIS.

remained intact. The leading capsule deformed principally at the impact end, but did not fail, as shown in Fig. I-7. The maximum diametral and height strains were 5.8 and -6.6%, respectively. There was no evidence of large local strains. The trailing capsule GCI-40 exhibited a maximum diametral strain of 2.6% and a height strain of -1%. The strain levels in the leading capsule IRG-59 are similar to those observed previously for double 0° impacts without aeroshells (see Table I-1), suggesting that the CBCF insulation adds no impact protection.

b. DAGCI-0-P1. This was a double impact at 0° (end-on) similar to DAGCI-0-C1, except PG was used as an insulator instead of CBCF. The GIS wall thicknesses and standoff design were similar to DGIS-12. The two PG liners were 0.77 mm thick, of LMRC design. All other details of assembly and preparation were similar to DAGCI-0-C1. The assembly before impact is shown in Fig. I-8. The leading capsule was IRG-61, Ir-0.3% W, with a $^{238}PuO_2$ fuel pellet of 85.1% theoretical density. The trailing capsule was GCI-21, Pt-3008 with a UO_2 fuel simulant.

The gas gun fired prematurely during this test at a breech pressure of<30 psig instead of the typical 128 psig. The capsule temperature was ~600°C at the time of firing and the velocity well below the intended 58 m/s. Very little

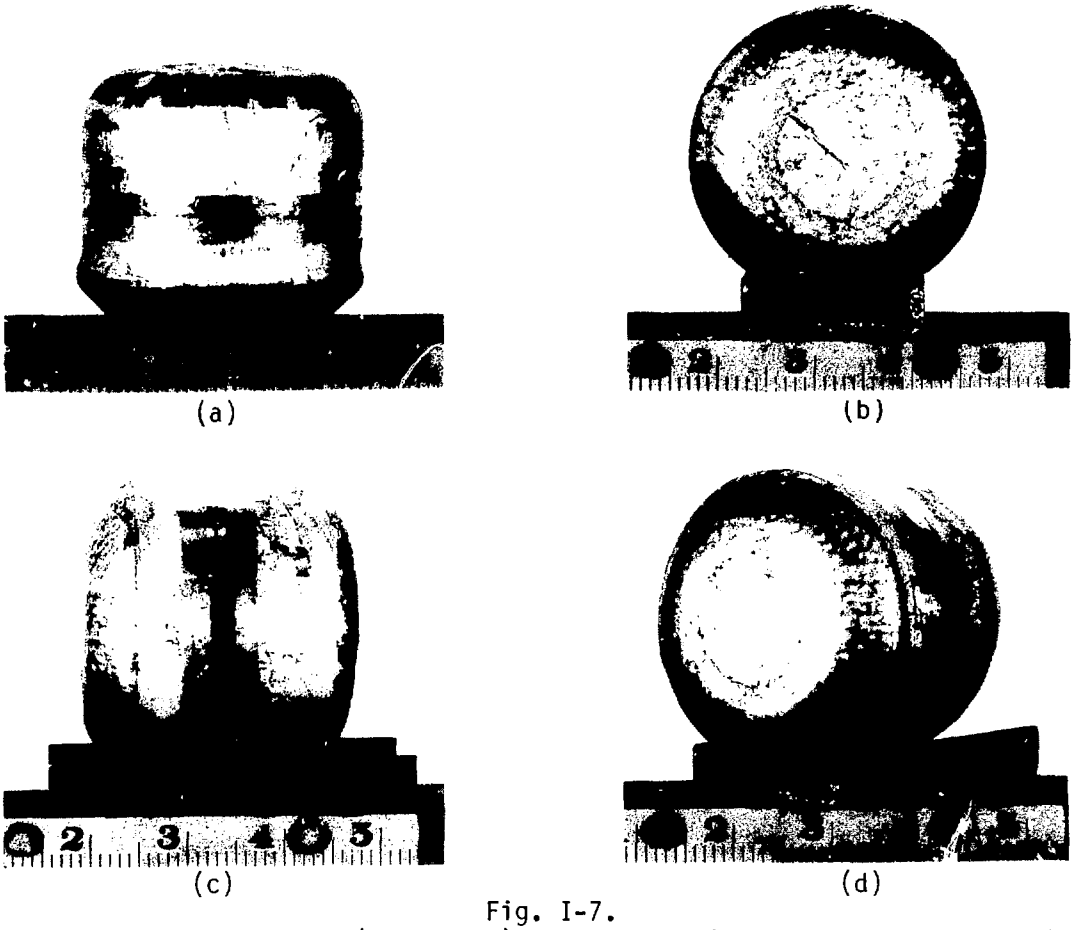

Fig. I-7.
DAGCI-O-C1: Capsule IRG-59 (Ir-0.3% W) was the leading capsule in this double impact at 0°, 58.3 m/s, and 965°C. (a) Side profile, (b) impact end, (c) side profile at 90°C, and (d) oblique view.

deformation occurred in the aeroshell and the capsule strains were 2.9% diametral and -3.3% height. Because of the misfire, we are not able to compare the PG design to the CBCF design in the 0° orientation.

c. DGIS-O-R2-23. Microstructural work has been completed on capsule IRG-48 used in this test. This double end-on test utilized capsule IRG-48/PuO_2 and GCI-27R/UO_2, at a temperature of 965°C and a velocity of 57.7 m/s. The test was preceded by a 1700°C reentry heat pulse.

Follow-on capsule GCI-27R/UO_2 was not deformed to any significant degree, but the leading capsule (IRG-48) was subjected to considerable gross deformation and severe local deformation in shear at two "pusn-through" sites. The only fracture was a crack at one "push-through, as shown in the November monthly report.

A complete cross section of the capsule is shown in Fig. I-9 and typical microstructures of various regions of it are shown in Fig. I-10. In general, the capsule appears to have been of high quality; the weld shows uniformly

TABLE I-1

IMPACTS OF 62.5 W Ir-0.3% W/PuO_2 Capsules

Capsule Number	Type of Impact	Capsule Location	Heat Treat and grains/thick	Impact Shell	Impact Temp. (°C)	Impact Velocity (m/s)	Max. Diam Strain %	Diagonal or Diametral Shrinkage %	Max. Positive Weld Strain	Local Strains		
										Shear or Thickness	Bending	Fracture
IRG-10	Double 90°	Leading Caps.	1h at 1500°C 25-28	DGIS-2	965	58	2.5	-1.3	4%	a	<5%	No
IRG-30	Double 0°	Leading Caps.	-"-	DGIS-6	965	58.1	5.5	-6.6 (Height)	4.3	46%	16	No
IRG-17	Module 45° Edge	Leading GIS	-"-	DGIS-2	965	58	9.0	-12.4	8.9	40	15	No
IRG-4	Double 27°	Leading Caps.	-"-	DGIS-2	965	57.2	3.5	-8.9	3.5	a	9	No
IRG-26	-"-	-"-	-"-	DGIS-2	965	56	9.3	-7.6	8.1	75	20	No
IRG-23	-"-	-"-	-"-	DGIS-4	965	57.9	5.8	-7.9	5.8	a	15	No
IRG-24	-"-	-"-	-"-	DGIS-5	965	58	5.1	-8.3	5.1	a	8	No
IRG-27	-"-	-"-	-"-	DGIS-6	965	58	4.3	-7.7	4.3	24	9	No
IRG-33	-"-	-"-	-"-	DGIS-6	965	58	8.8	-9.2	8.8	a	<16	No
IRG-42	-"-	-"-	1h at 1650°C	DGIS-6	960	58	4.1	-6.8	4.1	a	10	No
IRG-19	Module 45° Short Edge	Leading GIS Leading Caps.	1h at 1500°C 25-28	DGIS-3	965	57.6	4.6	-9.3	4.1	a	13	2 massive microcracks
IRG-20	-"-	Trailing GIS Leading Caps.	-"-	DGIS-3	965	57.6	3.0	-2.4	2.8	a	<5	No
IRG-29	Module 45° Corner	Leading GIS Leading Caps.	-"-	DGIS-6	965	53	6.7	-7.1	5.0	a	16	No
IRG-28	-"-	Trailing GIS Leading Caps.	-"-	DGIS-6	965	58	0.8	-1.7	0.8	a	<5	No
IRG-14	Double 27°	Leading Caps.	1h at 2800°C 5-6	DGIS-6	800	59.0	~10	Could not be measured	~10	b	b	Yes catastrophic
IRG-40	Double 27°	Leading Caps.	2½h at1500°C 13-14	DGIS-7	1075	71.9	17	-11.7	17	~90	20	Push-through failures
IRG-37	Double 27°	Leading Caps.	20h at 1500°C 13-4	DGIS-8 Std. Thick	1075	58	10.4	-14.6	10.4	a	6	No
IRG-50	Double 90°	-"-	-"-	DGIS-9 Std. thick	1075	58	+12.6 (length)	-13.0	9.7	a	11	No
IRG-51	Double 0°	-"-	-"-	DGIS-10 Std. thick Inc holes	965	56	6.0	-7.3	b	a	b	No
IRG-25	Double 0° w/TZM	-"- TZM follower	1h at 1500°C 25-28	Half GIS No holes	965	58	5.7	-2.5	b	a	7	No
IRG-26	-"-	-"- TZM follower	-"-	Half GIS 40% holes	965	58	4.4	-2.7	b	b	b	No
IRG-44	Double 27°	Leading Caps.	20h at 1500°C C + 170°C Reentry	DGIS-12 Bulk Liner	965	58	10.6	-6.4	9.2	b	b	No
IRG-48	Double 0°	-"-	20h at 1500 C + 1700°C Reentry	DGIS-13 (GCI-1 PG Ring	965	57.7	7.3	-8.0 (Height)	6.9	severe	severe	Yes
IRG-49	Double 27°	-"-	-"-	-"-	965	58.1	10.9	-13.9	11.4	severe	severe	Yes
IRG-59	Double 0° with Aeroshell	-"-	20h at 1500°C + 1700°C Reentry	DGIS-14 CBCF	965	58.3	5.8	-6.6 (Height)	5.1	a	b	No
IRG-60	Double 45° with Aeroshell	-"-	-"-	DGIS-14 CBCF	965	59	6.5	-9.2	5.9	b	Significant	No
IRG-64	-"-	-"-	20h at 1500°C + 1h at 1100°C	DGIS-12 PG	965	58	3.1	-5.5	3.1	a	a	No
IRG-57	Double 27°	-"-	20h at 1500°C + 1h at 1100°C	DGIS-12 Bulk Liner	965	58	8.4	-9.5	8.4	b	severe	Yes

[a] Not significant

[b] Not yet measured

complete but not excessive penetration and good dimensional control (but with a nearly continuous perpendicular grain boundary that represents a plane of weakness); the grain size is small (but nonuniform, showing some incompletely recrystallized areas); and the overall finish is excellent.

d. DGCI-27-R3-23. Microstructural work has been completed on capsule IRG-49. This double 27° impact utilized capsule IRG-49/PuO_2 and capsule GCI-25R/UO_2 and was carried out at 58.1 m/s and 965°C. The test was preceded by a 1700°C reentry heat pulse.

Follow-on capsule GCI-25R/UO_2 was not significantly deformed by the impact test, but leading capsule IRG-49 had large overall deformations and severe local deformations at the impact face. Several push-through shear areas were observed, with one resulting in capsule failure. The external appearance of IRG-49 was

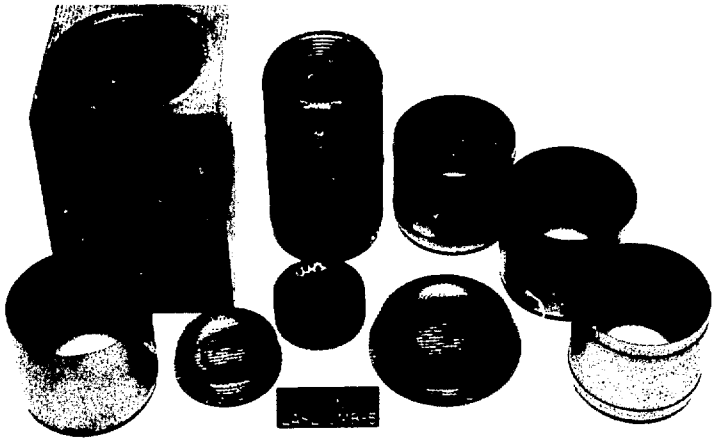

Fig. I-8.
DAGCI-0-P1: Aeroshell PG insulator and double GIS for this double 0° impact. Test misfired at low velocity and low temperature.

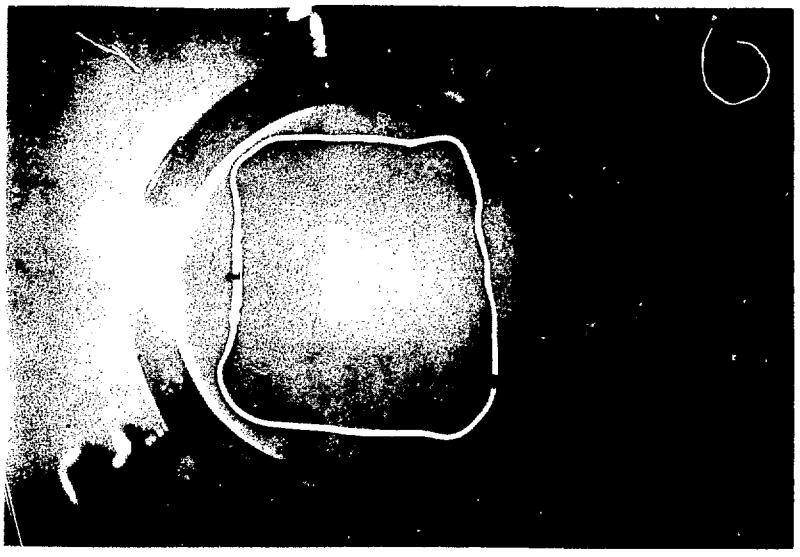

Fig. I-9.
IRG-48 after impact. The capsule was sectioned longitudinally. The gap on the impact face is an artifact of the fuel-recovery procedure and is not related to the impact event. 1.35X.

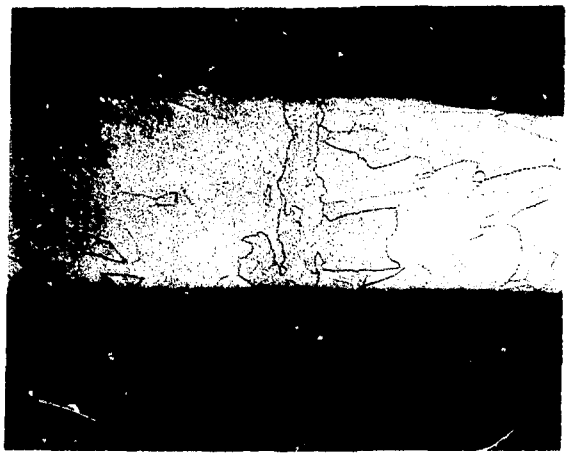

(a)

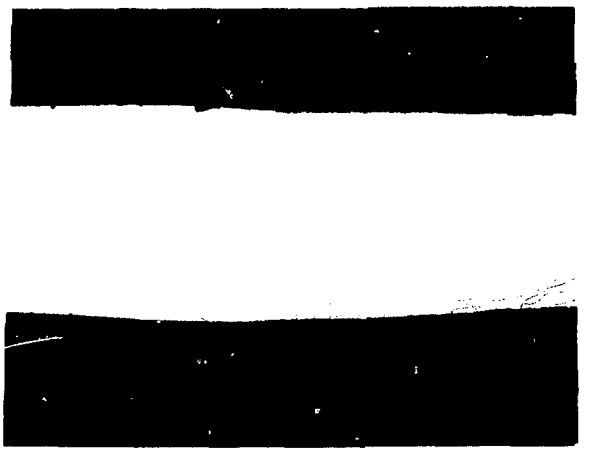

(b)

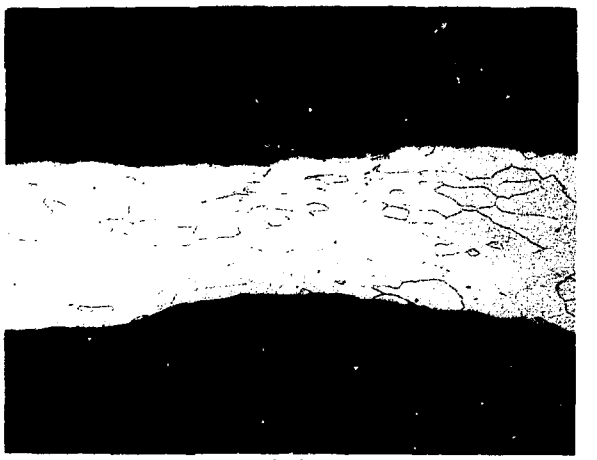

(c)

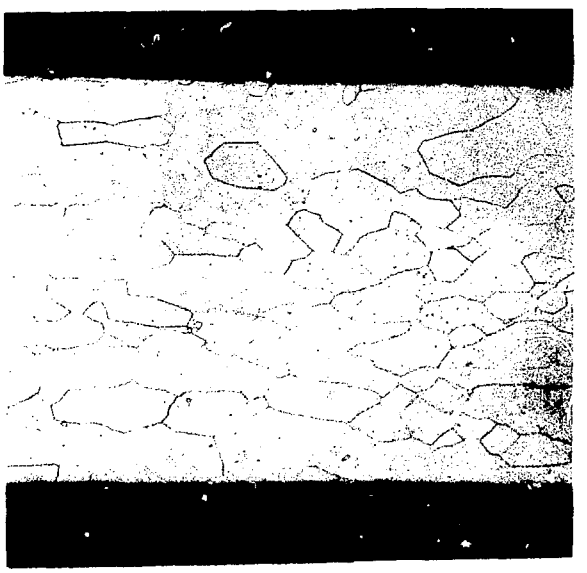

(d)

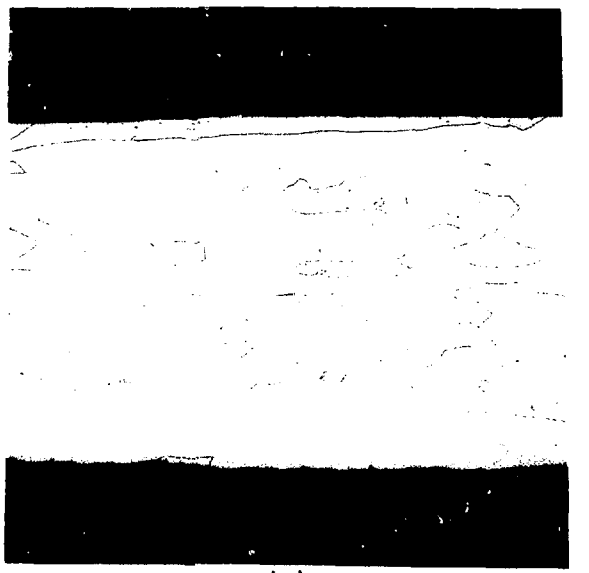

(e)

Fig. I-10.
Post-impact photomicrographs of the cross section of IRG-48: (a) microstructure of closure weld at 1-diam. of the cross section, 40X; (b) microstructure of closure weld at other diameter, 40X; (c) microstructure of a thinned portion of the capsule wall, 50X; (d) an illustration of an atypical grain structure, 100X; and (e) an illustration of a typical portion of the capsule wall showing incomplete recrystallization. Such behavior suggests inhomogeneities in composition, strain, or temperature (unlikely in such a small part).

illustrated in the November report, the cross section is shown in Fig. I-11, and microstructural features of the capsule are illustrated in Fig. I-12. Unfortunately, it is not always possible to reconcile the location of the cross section with all of the interesting features of a given capsule, therefore, we have no photomicrograph of the push-through crack that caused actual capsule failure. Again, as was the case for IRG-48, IRG-49 seems to have been a capsule of good quality with no obvious defects, therefore, it seems reasonable to conclude that the failures must have resulted from some specific test conditions. Whether the test hardware was responsible for creating conditions favorable to formation of large sharp fuel fragments, or whether the fuel pellets were predisposed to break up the mode is not yet known.

C. Fuel Development

1. Fabrication. Four $^{238}PuO_2$ GPHS pellets were encapsulated in Ir-0.3% W for testing. Capsules IRG-60 (pellet GP24) and IRG-61 (pellet GP29) were cleaned by successive immersions in 3 acid solutions (5/2/2 of $H_2(HNO_3/HF)$ followed by immersions in water and ethanol. These capsules were cleaned to zero counts per capsule (swipe) and then transferred for testing.

Capsules IRG-41 (pellet GP44) and IRG-65 (pellet GP47) could not be cleaned after welding because they leaked at the outer rim of the vent covers. Both capsules will be opened and the vent areas will be examined metallographically. The pellets will be reencapsulated for testing.

To date, 32 $^{238}PuO_2$ GPHS pellets (62.5-W size) have been encapsulated for testing.

2. Microstructural Examination. Samples of the fuel pellets from three impacted samples were subjected to ceramographic examinations. In addition, an unimpacted fuel pellet was sectioned and examined. In the impacted cases, the capsules were opened with a minimum of physical disturbance of the contents so that fragments could be selected and identified with certainty. As a result, the fuel was not subjected to fines analyses.

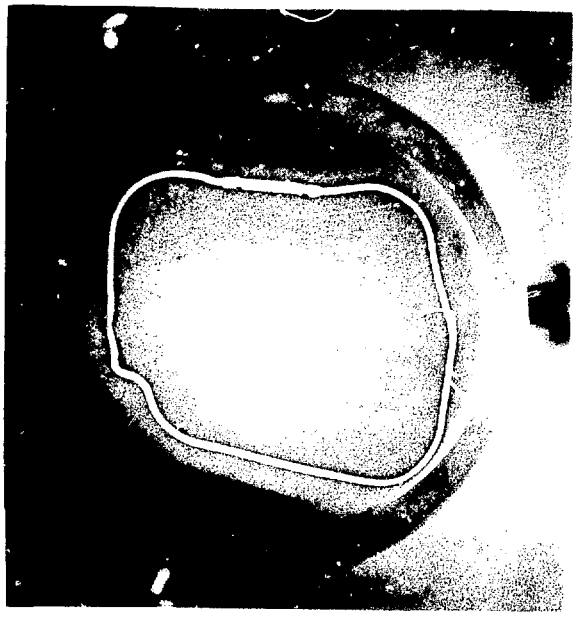

Fig. I-11.
Cross section of IRG-49 after impact. The section exposed does not intersect the failure, 1.3X.

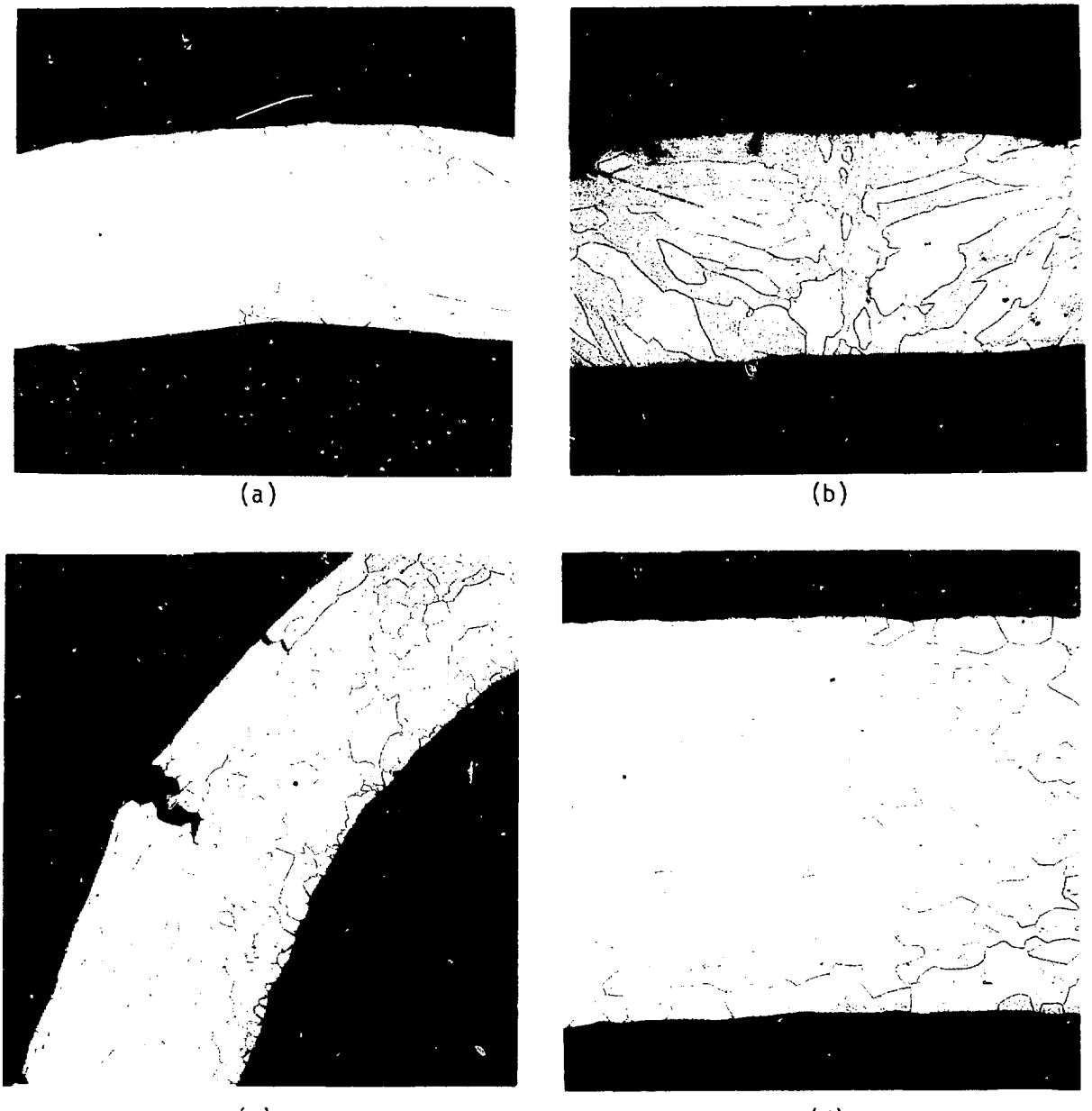

Fig. I-12.
Post-impact photomicrographs of the cross section of capsule IRG-49: (a) Microstructure of the closure weld at one diameter of the cross section, 50X; (b) microstructure of the closure weld at the other diameter, 50X; (c) an intergranular crack at the reverse bend near the "push-through" site, 50X; (d) a typical area illustrating grain structure and size, 100X.

a. GP-32. This pellet was from IRG-44, impacted at 58 m/s and 965°C, at 27° following a 1740°C reentry heat pulse. The iridium capsule was severely deformed but did not rupture (December report). Figure I-13 shows the important microstructural features of the fuel at the outside edge, about midway on a radius, and near the center.

b. GP-37. This pellet was from IRG-48, impacted at 57.7 m/s and 965°C, in the end-on attitude, following a 1700°C reentry heat pulse. The iridium capsule was severely deformed and failed by "push-through", as shown in the December report. Figure I-14 shows that the porosity gradients and distributions are similar to those observed in many other GPHS fuel pellets.

c. GP-38. This pellet was from IRG-49, impacted at 58.1 m/s and 965°C at the 27° attitude, subsequent to a 1700°C reentry heat pulse. The iridium capsule was severely deformed and suffered several minor "push-through" cracks. Figure I-15 illustrates the general break-up of the fuel pellet, and Fig. I-16 illustrates the microstructural features of GP-38.

d. GP-50. Los Alamos Scientific Laboratory (LASL) GPHS pellet GP-50 was sectioned in order to compare its "as-fabricated" structure to that of LASL pellet GP-31, which had been sectioned earlier by Savannah River Laboratory (SRL), and with the "post-impact" samples ordinarily utilized. The apparatus used for sectioning was a Buehler Isomet diamond saw, in conjunction with some simple jigs and fixtures made for the task at hand.

Figure I-17 presents views of the two faces of pellet GP-50 exposed by the initial diametral cut and the second, longitudinal cut. It is obvious that cracks, both radial and longitudinal, are present in profusion. We cannot be certain that the crack patterns shown in Fig. I-17 are the same as were present before cutting began, but we can say that the crack patterns are quite different from those of sectioned SRL pellet 7.

It seemed obvious from the crack density that a thin section of GP-50 could not be removed as a coherent slice, therefore, a woven glass fabric tape with a polymerizing adhesive was placed on a cut surface and a thin (~0.070") slice was cut while held on the glass-tape backing. This composition was mounted, ground, and polished, but a good finish was never obtained because of the independent shifting and tilting of individual fuel fragments. Nonetheless, the general microstructural pattern was obvious: a surface "rind" of low density that merged with a zone of significantly higher density that in turn gave way to a zone of slowly decreasing density. A photomacrograph of the slice is shown in Fig. I-18 and the pore structures are illustrated in Fig. I-19.

Essentially identical pore structures have been revealed in the many "post-impact" samples taken in the past years. The "new" information proved by the current exercise provides a strong suggestion of extensive cracking, which was present in the LASL pellet sectioned by SRL, but not in the SRL pellets sectioned by them. Comparisons of the impact behaviors of the two fuels are necessary in order to evaluate the responses of the two fuel microstructures.

C. Clad Development

The accumulated exposure time of the Pt-3008 vs $^{238}PuO_2$ (1100°C, vacuum) was 22 093 h, as of March 1, 1980.

D. Vent Behavior

During a simulated reentry heating pulse to 1700°C capsule IRG-58 swelled, which rendered the assembly unusual. This occurrence is unique in our experience. Investigations are under way to determine the cause.

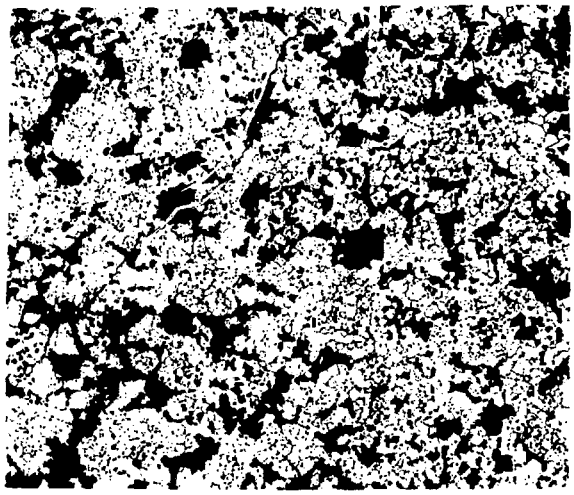

(a)

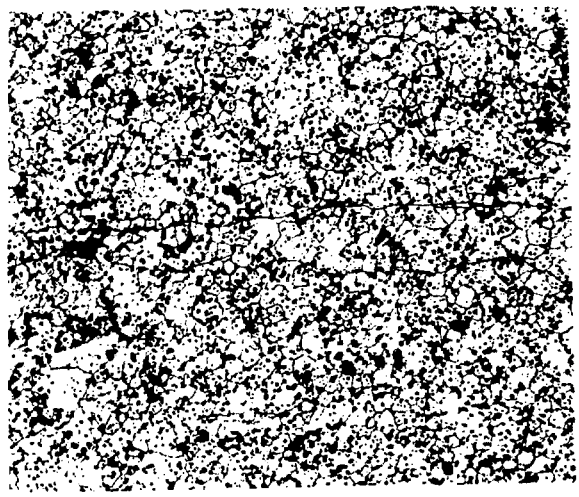

(b)

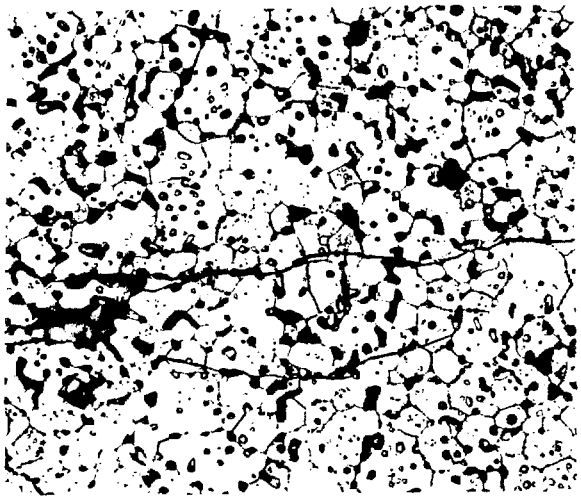

(c)

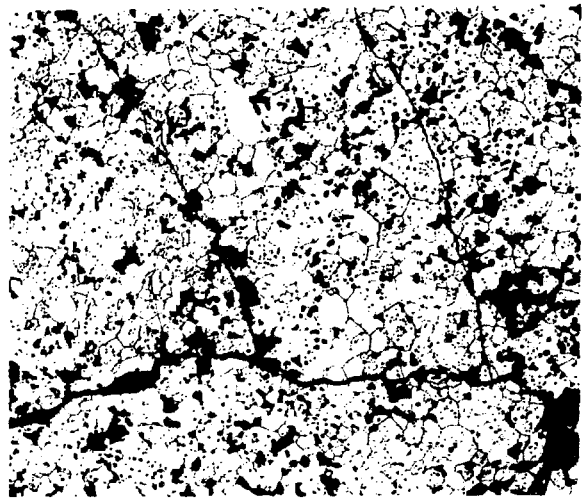

(d)

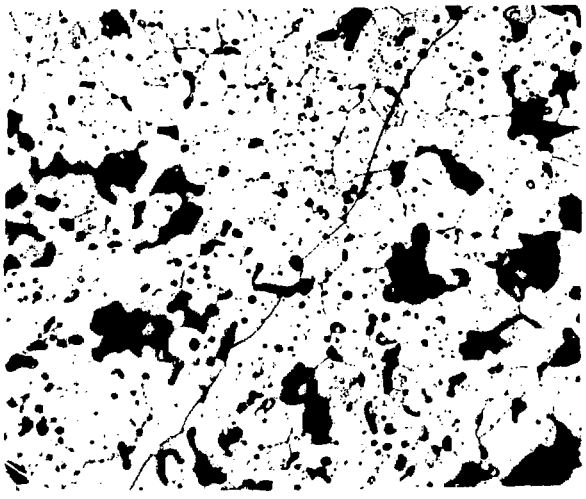

(e)

Fig. I-13.
Microstructural features of samples of fuel pellet GP-32. Samples were taken after impact. (a) Structure near outside edge of pellet, 100X; (b) structure near mid-point of a radius, 100X; (c) same as (b) but 250X; (d) structure near center of pellet, 100X; and (e) same as (d) but 250X.

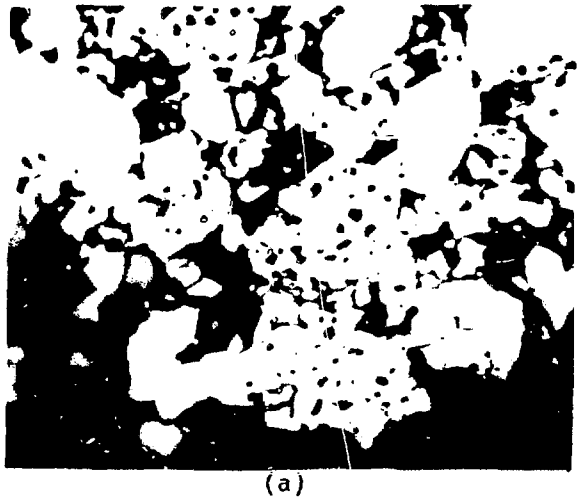

(a)

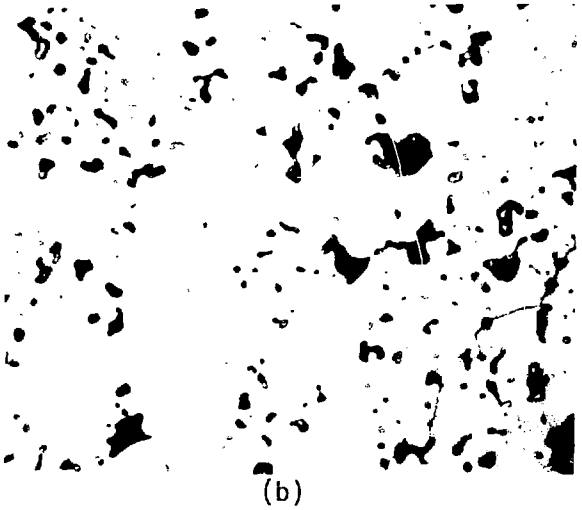

(b)

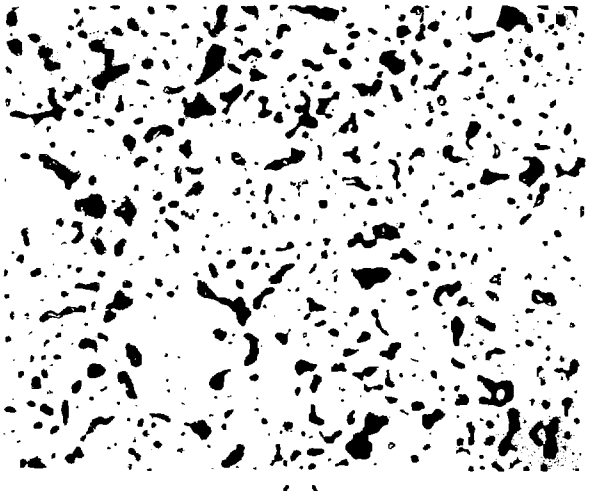

(c)

Fig. I-14.
Microstructural features of samples of fuel pellet GP-37. Samples were taken after impact. (a) Structure near outside edge of pellet, 250X; (b) structure near mid-point on a radius, 250X; and (c) structure near center of pellet, 250X.

Fig. I-15.
Fuel pellet GP-39 still in the capsule halves after opening, ~1X.

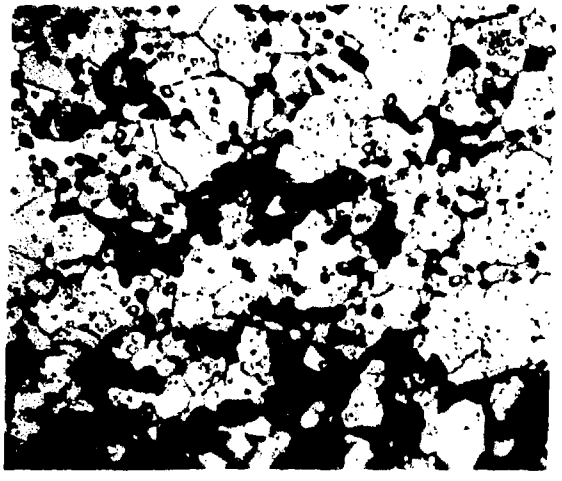

(a)

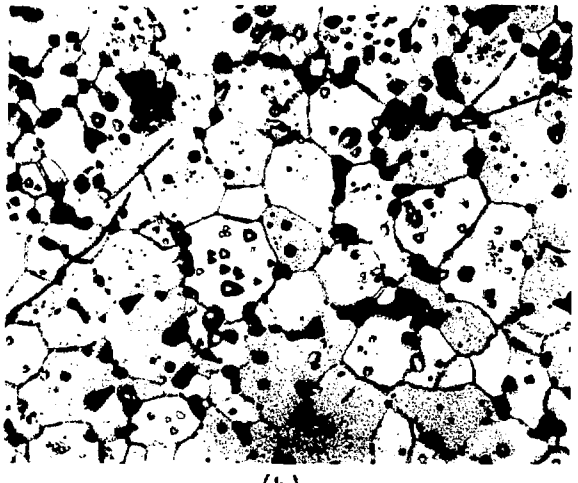

(b)

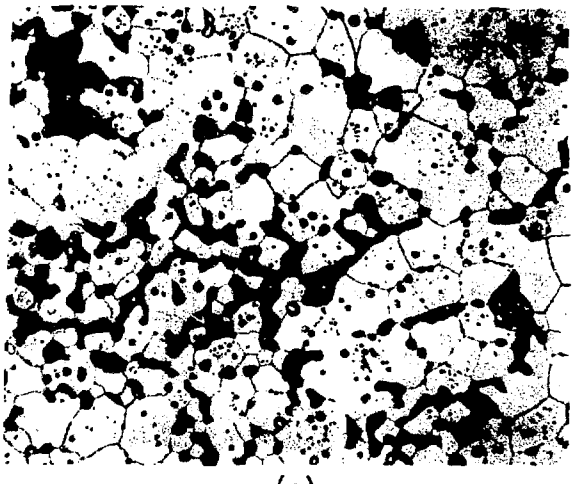

(c)

Fig. I-16.
Microstructural features of fuel pellet GP-38 after impact. (a) Near the surface, 250X; (b) about half the radius, 250X; and (c) near the center, 250X.

E. Vibration Testing

Machined FWPF components for Fairchild-Industries (FI) vibration tests were supplied by LASL. The FI mock-up tests were performed to establish a design basis for the CBCF insulator material. The tests were only intended to resolve the conflicting requirement of a mechanical stand-off between the FWPF GIS and the FWPF aeroshell without a prohibitive (heat-tap) thermal path to the clad of the fuel assembly. Insulator pieces of CBCF are protected from load bearing in the designs vibration tested at FI. However, it was established in those tests that small (~0.1 mm) clearances resulted in excessive CBCF abrasion losses. It is obvious that close attention to design and manufacturing tolerances are required to safely use the CBCF material in a GPHS module.

A complete graphitic assembly, made to the LMRC reference module design, was fabricated and transported for vibration tests at GE's Valley Forge Space Center. Mass drivers simulating the mass-volume equivalent of the clad fuel

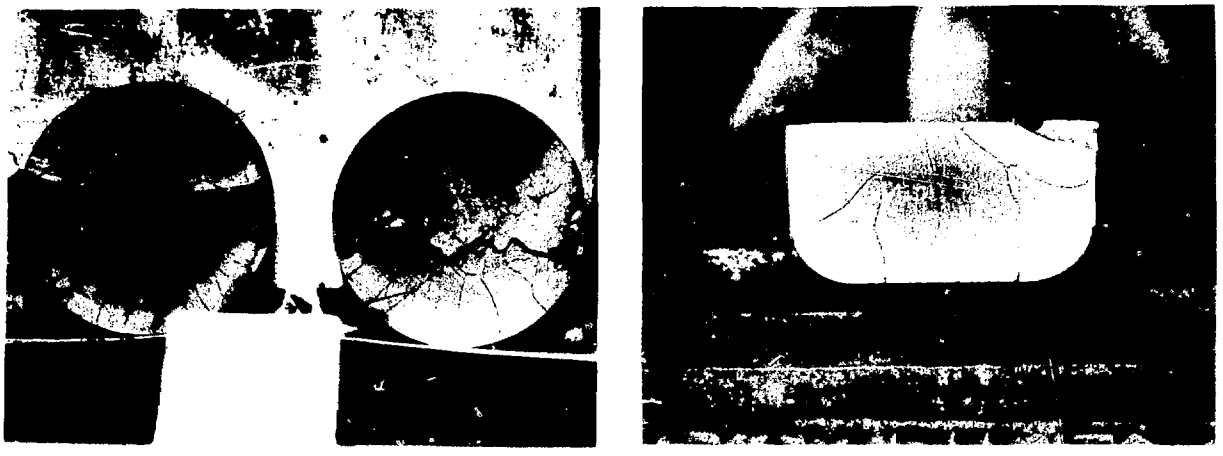

(a) (b)

Fig. I-17.
Fuel pellet GP-50, sectioned by a diamond saw, shows that large number of radial cracks (at this point) were more an assemblage of a large number of small fragments than a single coherent piece. (a) As-sectioned on a diameter; a high-contrast line on right-hand half is not a large crack but results from a difference in elevation and thus in shadowing because the cuts were not in perfect registry, ∿1.5X; and (b) a longtudinal section, ∿1.5X.

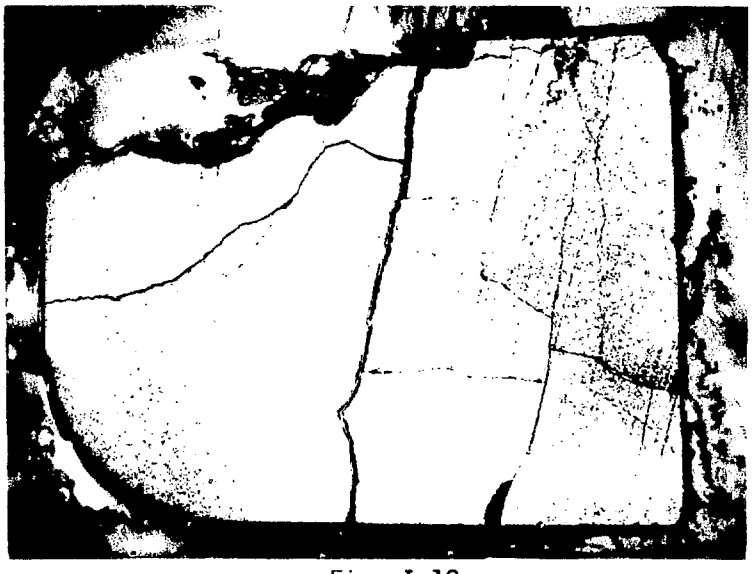

Fig. I-18.
Photomacrograph of a ground and polished thin section of GP-50. The differences in densities of various regions are quite visible, as is the general crack pattern. The bottom of the photograph is the bottom of the pellet, ∿8X.

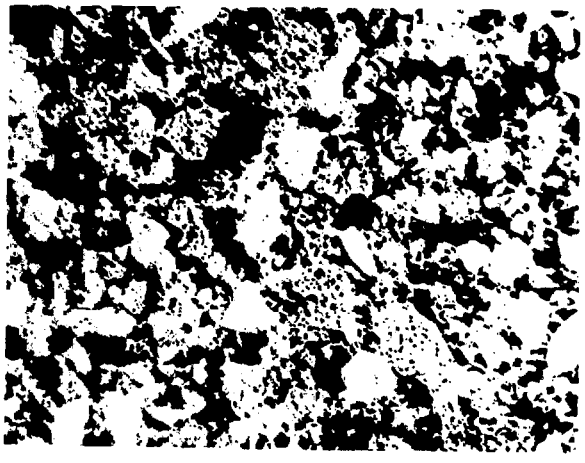

(a)

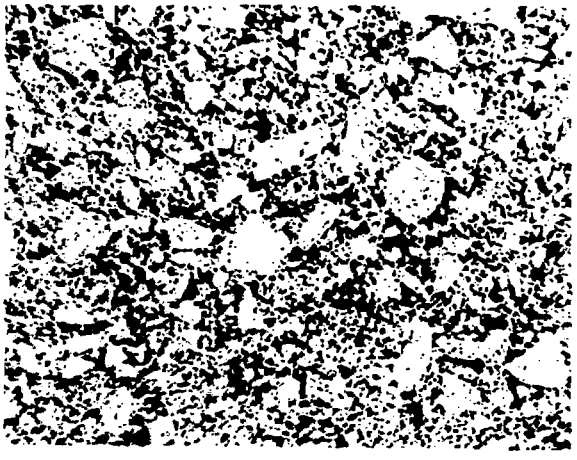

(b)

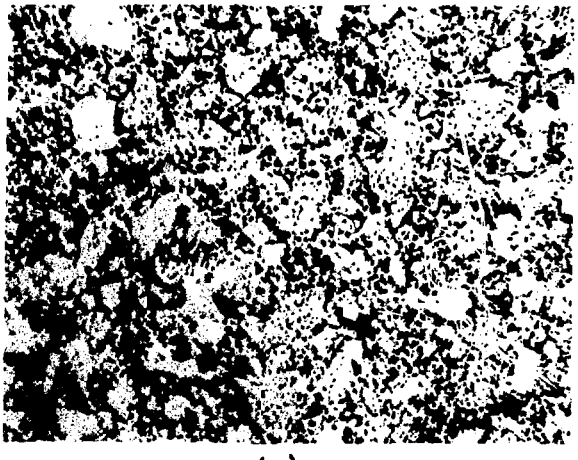

(c)

Fig. I-19.
Photomicrographs of different sections of the specimen section illustrated in Fig. I-18: (a) Pore structure at outer surface (T.D. is 65-70%), 100X; (b) pore structure near the region of highest density (T.D. is 85-90%), 100X; and (c) pore structure nearer the center of the specimen (T.D. is 80-85%), 100X.

assembly, were fabricated by GE for those tests. A sequential vibration test series to the up-graded vibration environment definition was performed. The module passed all the vibration test sequence without failure. A similar test will be made with the final CBCF-insulated design.

II. ENVIRONMENTAL STUDIES

A. Terrestrial Environments

1. Environmental Chamber Experiments. Six terrestrial environmental chamber experiments are under way as described in Table II-1.

The fragments of pressed plutonium oxide (PPO) greater than 6 mm in diameter (224 g) that resulted from the impact tests of MHFT-12 have been exposed to simulated humid weather conditions on loam soil for 2440 days. The environmental system was programmed for summer conditions (20 to 40°C, 87 to 95% RH) for 174 days, followed by 182 days under winter conditions (0 to 17°C, 71 to

TABLE II-1

TERRESTRIAL ENVIRONMENTAL CHAMBER EXPERIMENTS

Experiment Number	Description	Date Started
1	MHFT-12 chunks on loam; humid climate	6-21-73
3	MHFT-12 fines on loam, humid climate	9-27-73
6	MHFT-50 fines on loam; circular soil partitioner; humid climate	4-9-75
7	MHFT-27 fines on sand; arid climate	2-25-75
8	MHFT-50 chunks on loam; circular soil partiioner; humid climate	4-9-75
10	MHFT-27 chunk on sand; arid climate	2-26-75

100% RH). The system was then operated for 173 days of its second summer, 207 days of the second winter, 193 days of the third summer, 169 days of the third winter, 211 days of the fourth summer, 174 days of the fourth winter, 195 days in its fifth summer, 154 days in its fifth winter, 168 days in its sixth summer, 185 days in its sixth winter, and 178 days in its seventh summer, before being programmed for its seventh winter. The averages of the plutonium contents from liquid scintillation analysis and the volume measurements of the water that percolated through the soil for five 32-mm winter rains show decreased plutonium content, but little change in volume from last month (Table II-2). The average volume was 9.1 ℓ, compared with 8.9 ℓ last month, while the average plutonium content decreased from 1.6 to 1.2 μCi. The collection rate of plutonium in the dehumidifier condensate increased from 0.5 to 0.6 μCi/wk.

The finer fraction of MHFT-12, which consists of 28 g of PPO particles with diameters between 0.01 and 6 mm, was placed on loam soil and subjected to 110 days of humid summer conditions, followed by 147 days of humid winter weather. Subsequently, the seasons changed on the same days as in the chamber containing the large pieces. It has now been in its seventh winter for 74 days. The average of the measured volumes for five rains is higher, as is the average plutonium content (Table II-3). The average volume increased from 3.8 to 13.2 ℓ, the average plutonium content from 0.5 to 2.1 μCi. The collection rate for plutonium by the dehumidifier condensate decreased from 1.06 to 0.08 μCi/wk.

The fragments of PPO greater than 6 mm in diameter (221 g) from the impact test of MHFT-27 have been on sand in an environmental chamber programmed

TABLE II-2

PLUTONIUM IN PERCOLATED RAINWATER
(LARGE PIECES FROM MHFT-12)

No.	Date	Vol. Collected (ℓ)	Pu Found (μCi)
337	1/21	8.2	1.19
338	1/28	8.8	1.12
339	2/4	9.8	1.34
340	2/11	10.2	1.20
341	2/19	8.6	1.18
Average		9.1	1.21

for arid winter conditions (3 to 28°C, 21 to 87% RH) for 122 days, under arid summer conditions (26 to 53°C, 7 to 33% RH) for 196 days, under arid winter conditions again for 137 days, under arid summer conditions again for 211 days, in the third arid winter for 188 days, in the third summer for 181 days, 155 days in the fourth arid winter, 169 days in its fourth arid summer, 186 days in its fifth arid winter, 178 days in its fifth arid summer, and now in its sixth arid winter for 74 days. Liquid scintillation analysis and volume measurement of one 81-mm rain gave results of 0.56 μCi of plutonium in 14.0 ℓ, compared with 0.36 μCi in 11.2 ℓ last month. The collection rate for plutonium in the dehumidifier condensates was 0.18 μCi/wk, compared with 0.10 μCi/wk last month.

The finer fraction of MHFT-27, 34 g of particles of PPO with diameters between 0.01 and 6 mm, has experienced the same weather and soil conditions as the larger pieces. Volume measurement and liquid scintillation analysis of

TABLE II-3

PLUTONIUM IN PERCOLATED RAINWATER
(FINE MATERIAL FROM MHFT-12)

No.	Date	Rainfall (mm)	Vol. Collected (ℓ)	Pu Found (μCi)
329	1/21	32	16.5	2.7
330	1/28	32	13.0	2.2
331	2/4	32	14.4	1.7
332	2/11	30	11.4	2.2
333	2/19	30	10.8	1.9
Average			13.2	2.1

TABLE II-4

PLUTONIUM IN PERCOLATED RAINWATER
(LARGER PIECES FROM MHFT-50 ON COMPARTMENTED SOIL)

		Inner		Outer	
No.	Date	Vol (ℓ)	Pu (μCi)	Vol (ℓ)	Pu (μCi)
246	1/21	2.0	0.011	6.0	0.065
247	1/28	1.8	0.011	4.6	0.061
248	2/4	2.2	0.012	5.3	0.059
249	2/11	2.0	0.043	5.7	0.080
250	2/19	2.0	0.076	4.5	0.069
Average		2.0	0.031	5.2	0.067

water that percolated through the soil for one 81-mm rain gave results of 0.97 μCi of plutonium in 12.0 ℓ of water, higher in plutonium than the 0.18 μCi of plutonium in 6.4 ℓ of water for the last rain. The dehumidifier condensates collected 0.11 μCi/wk of plutonium, higher than the 0.08 μCi/wk last month.

The pieces (186 g) of PPO greater than 2 mm in diameter from MHFT-50 after an impact test have been on loam soil in an environmental test chamber programmed for humid winter conditions for 79 days, under humid summer weather for 193 days, under winter humid conditions for 169 days, under summer humid conditions again for 211 days, under winter humid conditions for the third time for 188 days, in the third summer for 181 days, in the fourth winter for 155 days, in the fourth summer for 167 days, in the fifth winter for 185 days, 178 days in the fifth summer, and now 74 days into the sixth winter. The soil in this chamber is divided into two compartments. A thin cylindrical 45-cm-diameter steel shell separates the central portion of the soil, which contains the PPO, from the outer portion. The rainwater that percolates through the soil in the two compartments is collected separately for analysis. In the liquid scintillation analysis and volume measurements of rainwater from five 23-mm rains, the average values for both compartments are lower this month except for the average volume of the inner compartment (Table II-4). In the inner compartment the average volume was 2.0 ℓ and the average plutonium content was 0.031 μCi, compared with 1.8 ℓ and 0.100 μCi last month. In the outer compartment the average volume decreased from 12.4 to 5.2 ℓ, the plutonium content from 0.18 to 0.07 μCi. The rate of collection of plutonium by the dehumidifier condensate decreased from 2.0 to 0.9 μCi/wk.

The fine particles (68 g) of MHFT-50, with particle diameters between 0.01 and 2 mm, have experienced the same weather conditions as the larger pieces and are also on loam in a similarly compartmented tray. Liquid scintillation analyses and measured volumes of percolated rainwater from five rains show a decrease in the average volume of the inner compartment and one high value in the outer plutonium (Table II-5). Otherwise the results were much the same

TABLE I. 5

PLUTONIUM IN PERCOLATED RAINWATER
(FINE MATERIAL FROM MHFT-50 ON COMPARTMENTED SOIL)

No.	Date	Rainfall (mm)	Inner Vol (ℓ)	Inner Pu (μCi)	Outer Vol (ℓ)	Outer Pu (μCi)
247	1/21	22	0.60	0.009	2.2	0.09
248	1/28	23	0.40	0.033	5.0	0.87
249	2/4	24	0.56	0.038	3.5	0.19
250	2/11	23	0.20	0.011	2.2	0.11
251	2/19	24	0.30	0.006	2.3	0.12
Average			0.41	0.019	3.0	0.28

as last month. The averages for the outer compartment volumes and plutonium contents are 3.0 ℓ and 0.28 μCi, respectively, compared with 3.2 ℓ and 0.104 μCi last month. The inner compartment averages are 0.41 ℓ and 0.019 μCi, compared with 1.3 ℓ and 0.015 μCi last month. The collection rate for plutonium in the dehumidifier condensate changed from 0.2 to 1.0 μCi/wk.

The experiment in which a 254-g sphere of plutonium dioxide clad with iridium and encased in a GIS, MHFT-23, was on sand under alternate winter and summer humid conditions for 1103 days was terminated April 17, 1978. A draft of the topical report for this experiment has been prepared and is being reviewed.

2. Terrarium Experiments. Chambers 5 and 9 have been fitted with fluorescent lights so that they can be used to measure plutonium uptake in growing plants and simple animals. A 24-h timer, wired to control the lights, was installed in each chamber and set in a summer cycle (sunrise at 7 AM and sunset at 8 PM). Blue grass was planted in each chamber, but two temperature excursions killed the grass in chamber 9. Baffles had been installed in the airstream of these chambers to reduce the effect of strong winds, which seem to be inimical to the growth of the grass, probably because of rapid drying of the soil. The grass has been cut regularly and the cuttings analyzed for plutonium to establish a blank, which is 0.5 pCi/g, a value that is probably not significantly different from our lower detection limit. An improved method of cutting the grass is being sought, preparatory to the introduction of plutonium. The grass in chamber 9 has been replanted and is growing. Equipment to correct the control problem in this chamber has been installed.

3. Soil Column Experiments. Three soil columns experiments are under way to test the transport of plutonium derived from plutonium oxide particles on the soil surface. The soil columns are made of silt loam soil, ∿ 14 cm high and 2.5 cm in diameter. These columns are identified as 7, 8, and 9. Column 7 has 3.5 mg of PuO_2 particles on its soil surface, with a particle size distribution mainly in the 40- and 60-μm range, column 8 contains 2.2 mg PuO_2 particles with

TABLE II-6

Pu TRANSPORT FROM PuO_2 PARTICLES

	Elution Duration			
	1091 days		1216 days	
Column	Total Vol (ℓ)	Total Pu (ng)	Total Vol (ℓ)	Total Pu (ng)
7	79.7	30.6	88.5	32.3
8	68.9	27.3	76.2	28.9
9	36.9	39.9	39.7	41.7

an average diameter of 12 μm, and 9 contains 2.6 mg with an average diameter of 7 μm. These three size ranges are from the same three batches of plutonia particles that we are using in the experiments for measuring dissolution rate as a function of particle size. The columns are being eluted with distilled water (a rainwater simulant). The columns have been in operation for 1216 days. Measurements made after 1091 and 1216 days of operation (Table II-6) show that the flow rates have not changed significantly. The variation in flow rate between columns is unexpected, inasmuch as they all contain soil from the same source. Radiation measurement show that at least 99% of the PuO_2 particles still remain at the top of each column; radiation cannot be detected from any particle that may move downward into the soil columns. Almost 90% of the plutonium found in the eluates was in the collection representing the first 5 days of operation. This was probably from the water suspensions of particles used to place the particles on the columns.

B. Aquatic Environments

1. Aqueous Release Rates As A Function of PuO_2 Particle Size. Three sets of sized $^{238}PuO_2$ particles, each having a different size distribution, are suspended in 1M $HClO_4$ in 50 mℓ volumetric flasks in a 37°C water bath. Periodically samples are removed, centrifuged to remove suspended particles, and then analyzed for plutonium. These data are needed to obtain information about dissolution under carefully controlled solution conditions and to determine the effect of particle size on dissolution rates.

The data (Table II-7) have been collected for 1561 days for the three particle size distributions. Each of these particle size distributions was used to prepare 4 experiments, 2 containing 2 mg of particles and 2 containing 10 mg. Distribution A consists of the largest particles, having a size range of ∿ 1 to 120 μm. Distribution B is intermediate in particle size and distribution C contains a preponderance of the smallest particles. The dissolution rates, grams dissolved/second (g/s), have changed only slightly during the past 3 months, and, as expected, the smaller particles release plutonium at a faster rate than the large ones.

A comprehensive review of this experiment, including a more detailed characterization of the three particle distributions, has been completed. The review revealed that the large particles in distribution A were actually aggregates of smaller particles. The suspension technique used in the particle

TABLE II-7

SUMMARY OF DISSOLUTION EXPERIMENT IN 1M $HClO_4$

Experiment Number	PuO_2 (mg)	Percent Dissolved	Dissolution Rate (g/s)	Dissolution Rate (g/s-g)
A1	2.02	4.9	7.3×10^{-13}	3.6×10^{-10}
A2	2.05	4.5	6.9×10^{-13}	3.4×10^{-10}
A3	10.19	4.6	3.5×10^{-12}	3.4×10^{-10}
A4	9.90	4.5	3.3×10^{-12}	3.4×10^{-10}
B1	2.02	8.1	1.2×10^{-12}	6.1×10^{-10}
B2	2.03	9.8	1.5×10^{-12}	7.3×10^{-10}
B3	10.25	8.8	6.7×10^{-12}	6.6×10^{-10}
B4	10.45	8.8	6.8×10^{-12}	6.5×10^{-10}
C1	2.23	18.5	3.1×10^{-12}	1.4×10^{-9}
C2	2.31	17.3	3.0×10^{-12}	1.3×10^{-9}
C3	9.89	18.4	1.4×10^{-11}	1.4×10^{-9}
C4	10.67	17.8	1.4×10^{-11}	1.3×10^{-9}

sizing produced a combination of "large particles" (did not suspend) and small particles thought to be individual members of aggregates that had broken apart. It is not possible to determine a quantitative estimate for the amount represented by the large fraction, therefore, the calculation of an available surface area is not possible.

Distribution B contained both large and small particles. In this case the large particles consisted of a preponderance of single large particles with some fines adhering to them, whereas the large particles in distribution A consisted of aggregates of similar size particles. Again, it is not possible to determine a total surface area because the sizing technique does not produce a quantitative estimate for the amount represented by each fraction.

Distribution C behaved normally in that all particles could be suspended and there were no anomalous large particles. This distribution lends itself to a calculation of total surface area but there is no assurance that the initial area has remained constant. In fact, it can be argued that the surface area has changed during the course of the experiment.

Grams dissolved versus time plots of representative experiments (A-1, B-1, C-1) exhibit no discernible discrepancies. Each plot shows increasing dissolution of $^{238}PuO_2$ with C-1 > B-1 > A-1. Integral dissolution rate plots show significant differences among the three experiments. A-1, coarse particles, has a shallow minimum at $\sim 3 \times 10^7$s, whereas B-1, medium size particles, has a low maximum at $\sim 2 \times 10^7$s. C-1, fine particles, exhibits a strong maximum $\sim 2 \times 10^7$s and has since decreased by 30%. The maximum is 3 times that of B-1. It can be postulated that the initial rapid increase in the dissolution rate of C-1 represents the solubilization of the smallest particles. The rate is now decreasing because of the reduction in surface area since only "larger" particles remain.

The third column in Table II-7 lists the percent of original material that has dissolved. Since a substantial amount of the original material has dissolved, ∿ 17% in the case of experiment C, the distribution of particles in each experiment may have changed considerably. An ultrafiltration echnique is being investigated whereby the size distribution in each sample may be determined. If the technique is successful part or all of the experiment will be terminated.

An extraction procedure, designed to extract only Pu^{+4}, is being applied to these experiments. Preliminary results indicate that the plutonium in solution is 90%, or greater, in the ionic form. Work is continuing in this area.

2. Fuel Form Exposures.

a. Seawater. The large 25-W pellet, HPZ-59-4, has been in cold seawater for 1958 days (Table II-8). Its release rate is 19 nCi/m^2-s, up 36% from last month.

The tidal simulation aquarium, using the 19-W source HPZ-186-4, has been under way for 856 days. The source is on sand in a st. inless steel tray that is lowered into the water and subsequently raised above the surface twice every 24 hours. Figure II-1 is a plot of plutonium concentration in µg/ℓ versus time for the tidal simulation experiment. On day 103 (point A on Fig. II-1) a crack was observed on the face of the source and on day 393 (B) the source had split into two pieces. By day 404 (C) the source had separated into seven pieces. On day 451 (D) the elevator motor failed and the source was left submerged in the seawater. On day 481 (E) a sample of the source was removed for metallurgical examination and five sand samples were obtained from the tray on the bottom of the aquarium. At the present time the source is fragmented into 30 or more pieces. Therefore, a calculation of release rate per unit area is not possible because there is no reasonable estimate of the source surface area. On the basis of its original area, the release rate is 60 nCi/m^2-s, up 7% from last month's value.

The five sand samples, taken from the four corners and the center of the tray, were analyzed for plutonium content. The results ranged from 55.1 µg to 26.2 µg with an average of 42 ± 12 µg. Based on this average and on the surface areas of the sand tray and the sand samples it can be estimated that there are 28 mg of plutonium on or in the sand.

The 18-W pellet HPZ-174 has been immersed in seawater at 10°C for 852 days. The release rate is 6 nCi/m^2-s, down 14% from the value for the last 4 months. This is the same system in which we maintained a live sea cucumber for 230 days.

b. Fresh Water. The 2.5-W pellet, HPZ-60-2, is part of a set of experiments to compare release rates from PPO in seawater and in fresh water. Its average release rate after 2165 days of immersion is 130 nCi/m^2-s, unchanged for the last two months. This is the second highest release rate observed in this set of PPO pellets.

The fastest release rate is shown by the 25-W pellet, HPZ-111-1, immersed for 1864 days at 10°C. Its average release rate is 380 nCi/m^2-s, down 3% from the value observed last month. The highest rates from PPO are found in 10°C fresh water, and the lowest in warm seawater. There is little, if any, rate difference caused by a 10-fold difference in power level.

c. Source Term. The plutonium release rates shown in Table II-8 are essentially minimum release rates in that the removal of plutonium by deposition

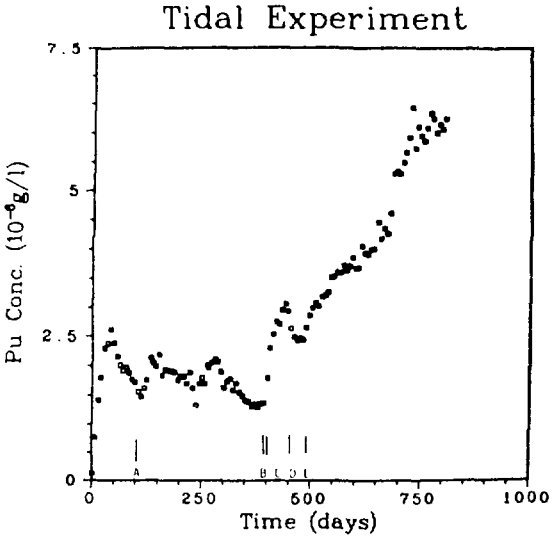

Fig. II-1.
Plutonium concentration in the Tidal Simulation Experiment.

on underwater surfaces cannot be measured. A total release rate, or source term, is not obtainable in an aquarium experiment. Therefore, a glass chamber was designed and constructed to permit such measurements.

This chamber is a 15.25-cm i.d. cylinder, 25.4-cm tall. It can be separated into two parts by means of an O-ring joint midway up the cylinder. The top half has a side arm for attaching a membrane filter, and an O-ring sealed port through which water samples can be withdrawn. The bottom half contains a glass pedestal for positioning the plutonium source.

A 48.6-g, bare $^{238}PuO_2$, source, HPZ-186-2, was positioned in an empty glass chamber on December 20, 1977, and the chamber was placed in an aquarium at 10°C for temperature control. This experiment will provide baseline data for an unclad source exposed to air only. Such conditions occur in some of the environmental chambers. The 0.05-μm pore-size filter is changed weekly and analyzed

TABLE II-8

SUMMARY OF
Pu RELEASE RATE FROM PPO IN AQUATIC ENVIRONMENTS

Sample	Power (W)	Immersion (days)	Water	Temperature (C)	Release Rate (nCi/m^2-s)
HPZ-60-2	2.5	2165	Fresh	10	130
HPZ-111-1	25	1864	Fresh	10	380
HPZ-59-4	25	1958	Sea	10	19
HPZ-174	18	852	Sea	10	6
HPZ-186-4	19	856	Sea (Tidal)	10	60

for ^{239}Pu. This experiment was terminated on day 454. Only 2 filters out of 63 had shown any plutonium, 6 pg on one and 2 pg on the other. Neither result was confirmed by subsequent filters and are, therefore, attributed to contamination from an unknown source external to the experiment. The source was transferred to a second chamber and the first chamber was resealed and transferred for analysis. The source in the second chamber was submerged in deionized water for 30 min and then removed. At this point the source fractured into three pieces and further experiments with this source were cancelled. The second chamber was resealed in preparation for analysis.

Analysis of the first chamber consisted of the quantitative recovery of the $^{238}PuO_2$ on the interior surfaces. This was accomplished using a HNO_3-HF leach followed by a wash with a decontamination solution. No residual activity could be detected on the surfaces available for monitoring.

The total ^{238}Pu recovered was 1.41 μg which represents a release rate per unit surface area of 22.1 pg/m^2-s. This number can be compared to the release rates seen in the aquatic environment experiments which vary from 0.59 to 36 ng/m^2-s. The analysis of the second part of the experiment in which the source was submerged indicated the release of 49.3 μg. Calculations based on the same surface area and a 30-minute submergency yields a release rate of 16.8 μg/m^2-s. This calculation may be invalid since the initial release may be that of loose material on the "old" surface of the source. The next experiment, that of the release from a "new" surface of the same source, could not be performed because the source broke into three parts.

Four experiments in glass chambers were initiated during this report period. Each experiment uses a GROG type source containing approximately 40.6 grams of plutonium. The four experiments consists of a fresh water and a simulated seawater environment at 10°C and at 35°C. Aerator tubes were installed in each chamber to maintain air-saturated conditions and to provide some stirring. The filters used on the 35°C experiments are 0.6 μm, whereas on the 10°C experiments, 0.05 μm filters are used.

Each source was installed in a glass chamber in a dry condition. After installation the chamber was sealed and a vacuum was applied to the filter. The chamber was then flooded with either fresh water or simulated seawater (approximately 2.3 ℓ). This procedure is expected to collect any plutonium released upon initial contact with the water.

3. Water Samplers. Two water samples were shipped to the Naval Ocean Systems Center at San Clemente Island. On May 15, 1979, the two samplers were attached to two cages and placed on the ocean floor. One sampler was placed in the Cermet area and activated by navy divers. The second sampler was placed and activated on the ocean floor approximately 60 feet NNE of the first unit. These two units were designed to collect 1.5 ℓ of water in 90 days. They have been received back at Los Alamos.

Sample #1 has been opened and the contents removed. Severe corrosion was observed on all four valves and a deposit was found on the interior walls and on the top of the piston. This deposit was easily removed with a water wash and a light rubbing. Samples of the interior deposit and samples of the deposit on the exterior of the sampler have been submitted for elemental analyses.

The total seawater sample obtained during the 3-month sampling period amounted to 440 mℓ. It was noted that the lower receiver had lost its vacuum. Corrosion of the vacuum valve may have resulted in this vacuum loss and subsequent equalization of the pressure on both sides of the piston which terminated sampling.

The 440 mℓ sample, the sludge deposit, and the tissue used to wipe the interior walls were treated with HNO_3-$HClO_4$. The resulting solution was highly colored (yellow) which produced considerable quenching during liquid scintillation counting. Therefore, the sample was split into five aliquots. Three aliquots were processed using a microporous anion exchange resin. The three samples processed by anion exchange gave values of 230, 13, and 19 d/m. The sample containing 230 d/m had been handled in an area where cross contamination was possible; therefore, this value was discarded. Blanks, processed through the complete anion exchange procedure, gave values of 20 and 23 d/m. Therefore, the two remaining anion exchange values are considered insignificant.

The two remaining aliquots, processed by a lanthanum floride precipitation procedure, gave values of 49 and 16 d/m. Blanks for these procedures are being processed at this time. The second sampler will be processed after blanks are established.

C. Analytical Studies of PuO_2-Soil Agglomeration

(Purchase Order LP9-3589K; LFE Environmental)

A progress report was not received from LFE Environmental this month as no samples were submitted to them for analysis.

Cumulative costs on this purchase order through January, 1980, were $5 752, leaving a balance of $7 828. This purchase order has been extended to a new termination date of September 30, 1980. Final payment of 3 775.68 was made on the previous purchase order, LP-8-8136D, for a total payment of $18 878.33 at close out.

III. SYSTEMS SUPPORT

A. Stirling Isotope Power System

The accumulated exposure time for the 800°C test assembly was 18 898 h as of March 1, 1980.

B. Multi-hundred Watt

1. Impact Tests.

a. MHFT-61. The fuel sphere assembly (FSA) of this test consisted of a DOP-26 iridium shell and an early Savannah River (SR) process development fuel sphere, designated HS-2,in a standard GIS. The FSA had been aged 8834 h at 1210°C (GIS). In view of the extended aging period, it was believed that an impact test of the assembly would yield data on the impact performance of DOP-26 iridium of value to the Galileo program.

Following a standard reentry pulse to an iridium temperature of 1550°C, the FSA was impacted at a velocity of 74 m/s and a post-impact containment shell (PICS) temperature of 1440°C.

The initial results of the post-mortem examination were reported in January. Briefly, no breach of the iridium was observed, the diametral strain was +6.9% and the height strain was -23.5%. Two linear fuel fragment punch displacements were noted on the impact face of the post-impact sphere assembly (PISA).

Metallographic examination of a cross section of the PICS through the weld indicated that severe iridium transport had occurred, resulting in complete destruction of the weld band as illustrated in Fig. III-1. Typical microstructures of the iridium hemishells are shown in Fig. III-2. The grain size was

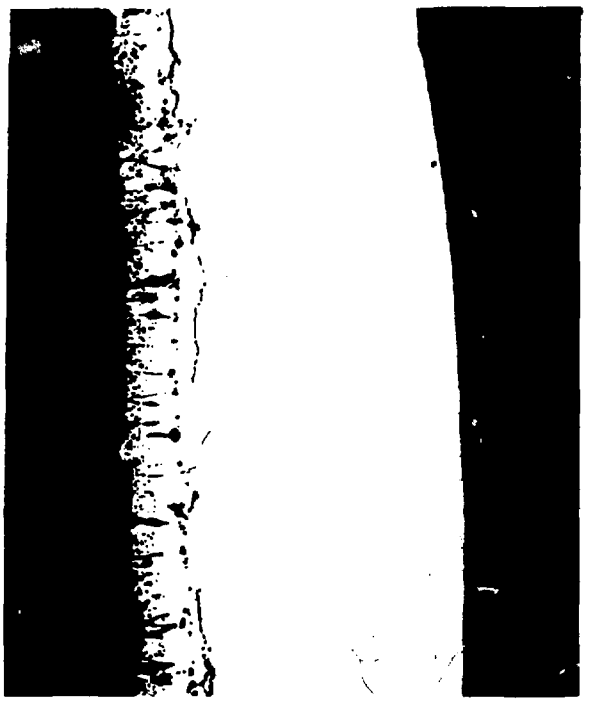

Fig. III-1.
Metallographic cross section through weld of MHFT-61.

(a) (b)

Fig. III-2.
Typical microstructures of the iridium PICS of MHFT-61.

Fig. III-3.
Metallographic cross section through a fuel fragment punch displacement on the impact face of the PICS of MHFT-61.

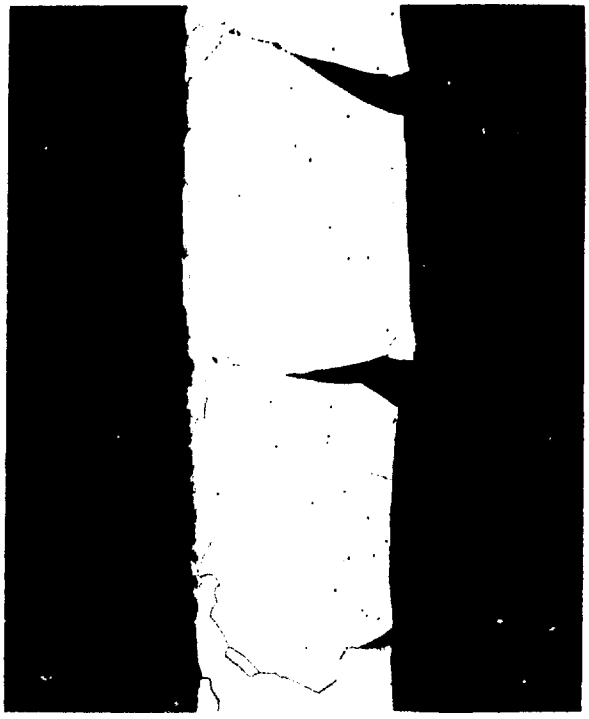

Fig. III-4.
Metallographic cross section through the fingerprint type cracks on the impact face of the PICS of MHFT-61.

nonuniform, varying from 1 to 6 grams across the thickness, with average values of 3.4 and 3.8 grains/thickness. The grain size predicted for this exposure by ORNL studies would be 9 grains/thickness. A metallographic cross section through one of the fuel fragment punch displacements is shown in Fig. III-3. It is evident that the iridium exhibited substantial ductility in this area, showing a reduction in thickness of 45%. Figure III-4 shows a metallographic cross section through the fingerprint-type cracks on the impact face. The cracks are intergranular, but were limited to about half the thickness of the iridium.

Metallographic examination of samples of the plutonia sphere from the impact face and the core showed the microstructure to consist of a uniform grain size with small, spheroidized, uniformly distributed porosity. No microstructural abnormalities were observed.

b. MHFT-67. This FSA was aged 100 h at a temperature of 1210°C (GIS) and impact tested at 83 m/s and 1440°C (PICS) following a reentry pulse to 1550°C. The aging treatment was selected to yield a condition that would indicate the performance of an assembly at "zero time" to provide a basis for comparison with the results obtained from subsequent impact tests of assemblies aged under conditions appropriate to the scheduled Galileo mission.

The assembly components were identified as follows:

Plutonia sphere	- HS-36
Iridium hemishells	- DOP-26
GIS	- 94664-2.

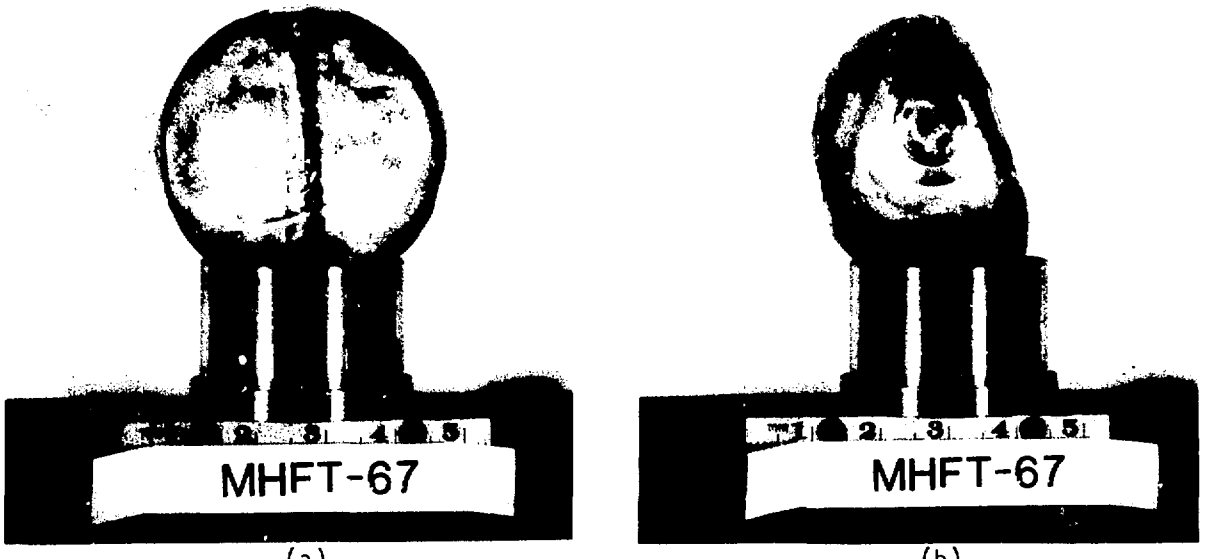

(a) (b)

Fig. III-5.
Photographs of the impacted PISA of MHFT-67: (a) Impact face and (b) profile view.

The cap of the GIS was oriented 180° to the initial impact point. Figure III-5 shows photographs of the impact face of the PISA and a profile view. A short linear fuel fragment punch displacement and an angular fuel fragment punch displacement were noted near the periphery of the impact face. The PICS was not breached at these locations and no fingerprint cracks were observed. The back side of the impacted PISA exhibited several locations indicating stretching of the iridium over corners and edges of fuel fragments, however, no cracks in the iridium were observed at these points. The indicated hoop strain was 7.4% and the height strain was -27.1%.

Typical microstructures of the iridium hemishells are shown in Fig. III-6. The average grain size, determined by an intercept method, was 14.2 and 14.8 grains/thickness, respectively. The predicted grain size for DOP-26 iridium treated for 100 h in vacuum, based on ORNL studies, would be greater than 18 grains/thickness. The metallographic cross section through the most severe of the fuel fragment punch displacements is shown in Fig. III-7. Good ductility of the iridium is demonstrated at this location. The reduction in thickness is 33%, based upon the thickness of the iridium shell on the impact face adjacent to the punch displacement.

No evidence of iridium transport was seen in any of the metallographic sections examined.

Bubble tests of the condition of the vent assemblies showed one vent open and one vent plugged. Metallographic examination of the cross sections through the vent assemblies revealed the presence of nonmetallic deposits in the iridium frit material, but the vent holes were free of extraneous material. The constituents of the nonmetallic deposits are being identified by electron microprobe analysis.

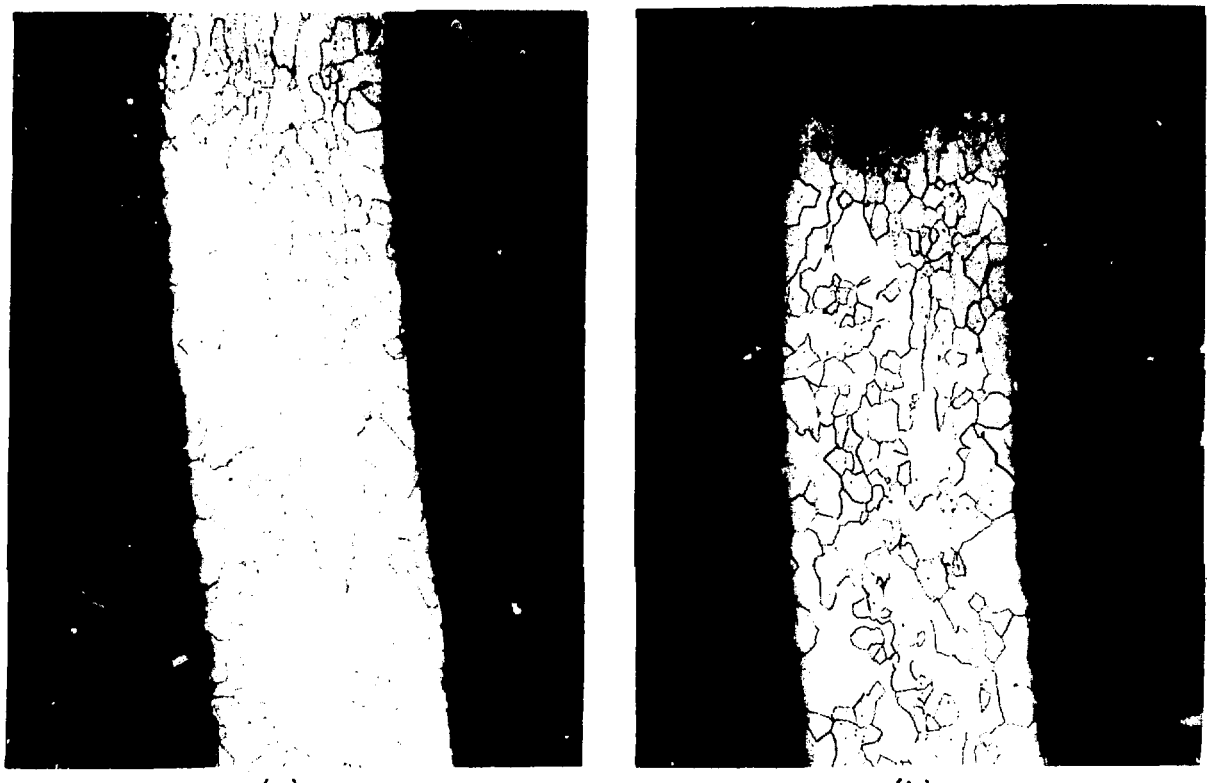

(a) (b)

Fig. III-6.
Typical microstructures of the hemishells of the PICS of MHFT-67.

Fig. III-7.
Metallographic cross section through a fuel fragment punch displacement on the impact face of the PICS of MHFT-67.

TABLE III-1

AES RESULTS FOR MHFT-66 (B3)

Specimen	Treatment	Location	Auger Intensity Ratios Th_{65}/Ir_{229}	P_{120}/Ir_{229}	C_{270}/Ir_{229}	O_{510}/Ir_{229}	S_{150}/Ir_{229}	Th_{65}/Ir_{43}
MHFT-66B3	HD Ir-0.3%W Aged 30 days in FSA at 1210°C GIS	Inside 150μm area	0.11	0	0.93	0.69	0.10	0.013
		Center	0.60	0.12	0.41	0.95	0	0.079
		Outside	0.50	0.12	1.15	1.11	0.13	0.078

2. Iridium Impurity Effects. One additional specimen of MHFT-66 (B3) was examined by Auger Electron Spectroscopy (AES). The results of this analysis of the grain boundary chemistry is shown in Table III-1. The concentrations of impurities were similar to those observed previously. The table summarizing AES results on recent FSAs is updated in Table III-2. We have examined six specimens of each FSA.

TABLE III-2

AES RESULTS ON RECENT MHW PICS (AVERAGE OF SIX AES SPECIMENS EACH)

		Th_{65}/Ir_{229}	P_{120}/Ir_{229}	S_{150}/Ir_{229}
MHFT-62	Inside	0.21	0	$0.3^{(2)*}$
	Center	0.48	0	$0.2^{(2)}$
	Outside	0.41	0	$0.3^{(2)}$
MHFT-64	Inside	0.37	0.09	$0.6^{(4)}$
	Center	0.63	0.16	$0.7^{(1)}$
	Outside	0.41	0.11	$0.5^{(3)}$
MHFT-65	Inside	0.20	0.66	$1.2^{(4)}$
	Center	0.52	0.43	$1.8^{(2)}$
	Outside	0.45	0.72	$0.9^{(3)}$
MHFT-66	Inside	0.27	0	$0.45^{(2)}$
	Center	0.54	0.05	$0.62^{(1)}$
	Outside	0.52	0.17	$0.42^{(2)}$

*Numbers in parentheses indicate number of specimens that exhibited a sulfur peak.

TABLE III-3

AES RESULTS ON P-DOPED Ir-0.3% W

Specimen	Treatment	Location	Th_{65}/Ir_{229}	P_{120}/Ir_{229}	C_{270}/Ir_{229}	O_{510}/Ir_{229}	Si_{92}/Ir_{229}	Th_{65}/Ir_{54}	S_{150}/Ir_{229}
OLMF-8-5	18h at 1500°C in vacuum + 1h at 1500°C with P_2O_5	Edge 150 μm area	0.50	0.26	0.45	0.85	0	0.071	0
		Center	0.92	0.39	0.20	0.55	0	0.105	0
		Edge	0.64	0.39	0.34	0.90	0	0.090	0
OLMF-8-5	Same + sputtered a few atomic layers in AES unit	Edge	---	---	---	---	-	----	-
		Center	0.05	Trace	0.64	0.67	0	0.006	0
		Edge	---	----	---	---	-	---	-
OLMF-8-44A	1h at 1500°C with P_2O_5	Edge	0.74	0.53	0.20	0.63	0	0.094	0
		Center	1.02	0.48	0.10	0.20	0	0.110	Trace?
		Edge	0.90	0.66	0.17	0.47	0	0.103	0
OLMF-8-44A	Same + sputtered a few atomic layers in AES unit	Edge	---	----	----	----	-	-----	-
		Center	0.13	0.09	0.86	0.43	0	0.017	Trace
		Edge	----	-----	----	-----	--	-----	-
OLMF-8-44B	1 h at 1500°C w/P_2O_5 + 18 h at 1500°C in vacuum	Edge	0.73	0.64	0.41	0.90	0	0.088	0
		Center	1.00	0.76	0.10	0.40	0	0.122	0
		Edge	0.71	0.59	0.18	0.85	0	0.095	0
OLMF-8-44B	Same + sputtered a few atomic layers in AES unit	Edge	----	----	----	----	---	-----	-
		Center	0.17	0.04	0.91	0.66	0	0.022	Trace
		Edge	----	----	----	----	----	-----	-

We have run additional AES studies on phosphorous-doped Ir-0.3% W. OLMF-8-5 was taken from the section of material sent to Don David at Mound Facility (MF). It was annealed for 18 h at 1500°C in vacuum plus 1 h at 1500°C with P_2O_5 in the same furnace with the four tensile specimens sent to ORNL. The AES results are shown in Table III-3 and summarized in Table III-4. The thorium and phosphorous intensity ratios was 0.69 and 0.35, respectively. These levels are compared with other phosphorous treatments in the tables. Doping with phosphorus for 1 h at 1500°C results in thorium and phosphorous ratios of 0.86 and 0.52. An additional 18 h at 1500°C in vacuum (in a graphite crucible) results in enormous grain growth, as reported last month. The thorium and phosphorous levels remain very high. ORNL has reported that additional treatment in vacuum after phosphorous-doping reduces the phosphorous levels significatnly. This obvious discrepancy must be resolved. It is most likely associated with the type of vacuum environment.

Two more biaxial disks were tested to study the effect of phosphorus on impact ductility. One disk (L-25-4) was annealed for 18.75 h at 1500°C in vacuum plus 1 h at 1500°C with P_2O_5; the same treatment given to the ORNL tensile specimens. The other (L-30-2) was a control specimen annealed for 19.75 h total at 1500°C in vacuum. Both were tested in the biaxial punch test apparatus at 45 m/s and 1350°C. Unfortunately, the circle grids could not be measured after deformation because they were not etched sufficiently deeply. However, both specimens exhibited substantial ductility (estimated fracture strains >70%)

TABLE III-4

GRAIN SIZE AND AES RESULTS FOR P-DOPING EXPERIMENTS ON Ir-0.3% W

Specimen	Lot	Treatment	Grain Size # grains/thickness	Auger Intensities Th_{65}/Ir_{229}	Auger Intensities P_{120}/Ir_{229}
DOP-26	GPHS Lots	1h at 1500°C in vacuum[a]	25-28	--	--
DOP-26	GPHS Lots	19h at 1500°C in vacuum	13	--	--
DOP-26	Early DOP-26 Lot, (1977)	18h at 1575°C in vacuum	8.5	0.60	0
OLMF-8-65	OLMF-8	19h at 1575°C in vacuum	7.4	--	--
L-30-1	L-30	19h at 1575°C in vacuum	6.2	0.34	0
DOP-26	Early DOP-26 Lot, (1977)	18h at 1575°C with P_2O_5	5.6	0.81	0.40
L-30-5[b]	L-30	19h at 1500°C with P_2O_5	8.7	0.55	0.28
OLMF-8-61	OLMF-8	19h at 1500°C with P_2O_5	7.8	0.81	0.38
OLMF-8-44	OLMF-8	1h at 1500°C with P_2O_5	19	0.82	0.47
OLMF-8-44A	OLMF-8	-"-	19	0.89	0.56
OLMF-8-44B	OLMF-8	1h at 1500°C P_2O_5 + 18h at 1500°C in vacuum	4.7	0.81	0.66
OLMF-8-5	OLMF-8	18h at 1500°C in vacuum + 1h at 1500°C with P_2O_5	12.6	0.69	0.35

[a] All vacuum treatments were done in graphite crucibles.

[b] Average of those AES specimens

and ductile fracture. We estimate that the grain size of these specimens is on the order of 12-13 grains/thickness. AES analyses will be run to determine the level of phosphorous contamination at the grain boundaries. A previous biaxial disk with 6-8 grain/thickness also showed no embrittlement resulting from the presence of phosphorus. A third section of this disk (L-30-5) was examined by AES. The results are shown in Table III-5. The average phosphorous level of the three specimens is shown in Table III-4 to be 0.28.

We also attempted to dope Ir-0.3% W sheet with sulfur in a similar manner to that used in the phosphorous experiments. DOP-26S1 was annealed in a graphite crucible at 1500°C for 19 h with MoS_2. The AES results in Table III-5 show no pickup of sulfur at the grain boundaries. We will attempt other experiments for sulfur doping.

TABLE III-5

AES RESULTS ON Ir-0.3% W

Specimen	Treatment	Location	Th_{65}/Ir_{229}	P_{120}/Ir_{229}	C_{270}/Ir_{229}	O_{510}/Ir_{229}	Si_{92}/Ir_{229}	Th_{65}/Ir_{54}	S_{150}/Ir_{229}
C-83-58	19h at 1500°C with P_2O_5	Edge	0.70	0.27	0.38	1.04	0	0.088	0
		Center	1.18	0.45	0.15	0.50	0	0.136	0
		Edge	0.41	0.28	0.30	0.78	0	0.055	0
2C2-2651	19h at 1500°C with M_0S_2	Edge	0.60	0	0.69	0.92	0	0.085	0
		Center	0.36	0.09	0.63	0.95	0	0.053	0
		Edge	0.46	Trace?	0.68	0.92	0	0.066	0

IV. LIGHT-WEIGHT RADIOISOTOPIC HEATER UNIT (LWRHU)

A. Fuel

Two lots of 16-each chamfered RHU production pellets were hot pressed from <125-μm GROG-type feed granules seasoned at 1100°C (60 wt%) and 1600°C (40 wt%). The feed granules were processed from SR Lot 440, Run 906923 (LASL Lot 38) and SR Lot 440, Run 906922 (LASL Lot 39). The feed material is enriched at 83.5 at.% ^{238}Pu, thus the fuel pellets have a thermal inventory slightly in excess of 1.1 watts at the time of fabrication.

After the pellets were hot pressed, they were sintered for 6 h at 1527°C in flowing Ar-$H_2{}^{16}O$. Fabrication parameters and dimensions for pellet lot RU 6 are listed in Table IV-1. Data for pellet lot RU 7 are listed in Table IV-2.

B. Weld Development

To date, we have welded 11 RHU development capsules in order to determine the optimum parameters for tungsten arc-welding and non-vented endcap to a fueled Pt-30 Rh alloy RHU capsule. The weld is required to exhibit full penetration with a slight fillet (approximately 15 mil) at the inside of the corner joint. The weld is to be free of defects such as pores, cracks, and inclusions and the exterior profile is to be smooth and even around the circumference. Grain size is to be minimized. The weld should extend about 0.1 mm above the surface of the endcap so as to provide a stand-off between the capsule and the graphite.

The major variables employed for the developmental capsules are listed in Table IV-3. The first column lists the capsule number and the second column lists the weld current. The third column lists the values for t_1, the delay time between arc start and the start of capsule rotation. For all capsules the revolution rate was 3 rotations per second. The fourth column lists the values for t_2, the time between the start of capsule rotation and the beginning of downslope for the weld current. No pulsing was employed for capsule WD-1. The remaining capsules were welded using a 4 Hz pulse, which is more of a ripple, being ± 3A the weld current. After capsule WD-6 was welded, the electrode was moved slightly outboard with reference to the capsule for the remaining welds.

A brief summary of the metallographic results for the first 10 capsules follows:

TABLE IV-1

RHU PRODUCTION PELLET LOT RU6

Feed Material	<125-μm $^{238}PuO_2$ granules (Lot 39) seasoned at 1100°C (60 wt%) and 1600°C (40 wt%)
Hot-Press Parameters	1530°C for 15 min at 19.5 MPa
Post-Press Sintering	6 h at 1000°C plus 6 h at 1527°C in Ar-$H_2{}^{16}O$
Comments	16 chamfered pellets, feed enriched at 83.5 at.% ^{238}Pu

Dimensions

Condition	Diam (cm)	Length (cm)	Weight (g)	Density (% TD)
As Pressed	0.628±0.001	0.953±0.004	2.646±0.002	84.7±0.4
Sintered	0.623±0.001	0.945±0.004	2.665±0.002	86.7±0.4

TABLE IV-2

RHU PRODUCTION PELLET LOT RU7

Feed Material	<125-μm $^{238}PuO_2$ Granules (Lots 38 and 39) seasoned at 1100°C (60 wt%) and 1600°C (40 wt%)
Hot Press Parameters	1530°C for 15 min at 19.5 MPa
Post-Press Sintering	6 h at 1000°C plus 6 h at 1527°C in Ar-$H_2{}^{16}O$
Comments	16 chamfered pellets, feed enriched at 83.5 at.% ^{238}Pu

Dimensions

Condition	Diam (cm)	Length (cm)	Weight (g)	Density (% TD)
As Pressed	0.631±0.001	0.961±0.004	2.644±0.002	83.1±0.6
Sintered	0.623±0.001	0.949±0.004	2.662±0.002	86.2±0.6

TABLE IV-3

RHU WELD DEVELOPMENT PARAMETERS

Capsule No.	Current (A)	t_1 (s)	t_2 (s)	$^{238}PuO_2$ RHU Pellet	Comment
WD-1	24	95/60	175/60	-	Not pulsed
WD-2	30	80/60	80/60	-	
WD-3	32/34	95/60	80/60	-	2 segments
WD-4	32	95/60	180/60	-	
WD-6	32	95/60	165/60	RU2-11	
WD-7	30	105/60	175/60	RU2-12	Changed electrode position
WD-8	32	110/60	175/60	RU2-13	No shim
WD-5	34	90/60	175/60	RU2-14	
WD-10	36	90/60	175/60	RU2-15	
WD-11	40	90/60	175/60	RU2-16	
WD-12	39	100/60	175/60	RU3-3	

WD-1. The endcap was welded on in two sections. A longitudinal section through the continuous weld portion was examined. Except for a large gas bubble, both welds exhibited 100% penetration. The capsule appears to have rotated off-center during welding. The grain size in the TIG welds is larger (about 3X) than that in the electron beam weld made at MF.

WD-2. This capsule and all subsequent capsules were pulse-welded. The capsule was welded in 3 segments. The overlap area was fully penetrated, the continuous weld area was not. The capsules appears to have rotated off-center during welding. The grain size in the TIG welds is larger (2-3X) that in the EB weld.

WD-3. This capsule was welded in 2 sections (each 180° of arc), one at 32A and the other at 34A. Both welds penetrated 100%. Again, the capsule appears to have rotated off-center during welding. The grain size was larger (2-3X) than that in the EB weld.

WD-4. The capsule was sectioned longitudinally at 90° to the start/stop overlap. The weld penetrated fully. However the grain size was still larger (about 4X) than that in the EB weld. The hardness of the tubing was measured beginning 50 μm from the inside surface and continuing, at 100-μm intervals, to 50 μm from the outside surface. The average hardness was 168 ± 6 DPH. The average hardness near the center of the endcap was 156 ± 2 DPH. The combination of equiaxed grain structure and slight variations in hardness numbers suggests a well annealed state. MF has apparently developed a process that yields a capsule with a hardness number of about 170 DPH. LASL has achieved successful impact with a capsule with a hardness number of 290 DPH. A hardness specification between these numbers is probably acceptable, but the closer the number to 170 DPH, the greater the safety factor in impact.

TABLE IV-4

OPTIMUM WELDING PARAMETERS FOR RHU CAPSULES

Process	Automatic Gas Tungsten Arc
Torch Gas	75 vol% He/25 vol% Ar
Welding Speed	3s/rev
Welding Current	39 A
Welding Time	t_1 = 90/60 s
	t_2 = 175/60 s
Pulsation	4 Hz
Arc Gap	0.040 inches
Electrode Angle	60°C to horizontal
Electrode Position	45°C up and out from outer capsule corner

WD-6. This capsule was cross-sectioned between the stand-off and the weld in order to visually examine 360° of the weld. All of the weld was fully penetrated. Again, the capsule appeared to have rotated off-center during welding and the grain size was relatively large.

WD-7. The electrode was moved out closer to the edge of the capsule while maintaining a 40-mil gap. The capsule was sectioned between the stand-off and the weld in order to visually examine 360° of the weld. Full penetration was achieved in the overlap region but not in the continuous weld region. The capsule appeared to have rotated on-center during welding and the grain size was smaller than that obtained previously.

WD-5. The weld had fully penetrated through a 300° arc of the continuous weld. A 60° arc (30° on either side of the start position) exhibited almost but not quite full penetration.

WD-8. The area of the weld near the start position again was not fully penetrated, but less so than for WD-5. The remainder of the weld was fully penetrated.

WD-10. The results were similar to those for WD-8 except that the region of not full penetration was reduced. The grain size was smaller than for previous development capsules.

WD-11. The weld had fully penetrated for 360°.

The optimum welding parameters for the RHU capsules, based on examination of the development capsules, are listed in Table IV-4. One or two more development capsules will be welded and examined to confirm these parameters prior to welding the production pellets.

C. Capsule Alloy Hardness

In order to help establish hardness specifications for the LWRHU capsule materials, hardnesses were measured on a weld development capsule and on an impacted RHU capsule.

As indicated above, the hardness of weld development capsule WD-4 was measured. It was measured 50 μm from the inside of the tube wall and at 100 μm toward the outer surface. The average hardness was 168 DPH and the sequential values were 158, 167, 167, 162, 173, 168, 170, 168, and 179. The hardnesses measured near the center of the end cap and well away from the welds were 158, 152, 156, 158, and 156. The microstructures of both pieces consisted of the equiaxed grains of a well annealed material and the small variation in hardness numbers confirms this.

The hardnesses of the tube wall of an impacted capsule averaged 289 DPH on the rear, unimpacted portion and 275 DPH on the impacted face. The end cap had a hardness of 243 DPH. In this case, the microstructures consisted of elongated, unannealed grains.

D. Surface Temperature

The surface temperature of the LWRHU in ambient air (23°C) was measured on a unit assembled from a fueled weld development capsule, PG insulator components, and a FWPF aeroshell. A fine, sheathed thermocouple was spring loaded in an end-plug spanner hole and the unit supported on a CBCF insulating block, as shown in Fig. IV-1. Measurement of the thermocouple output over a several hour period indicated a surface temperature of 42.4 ± 1°C (107-110°F).

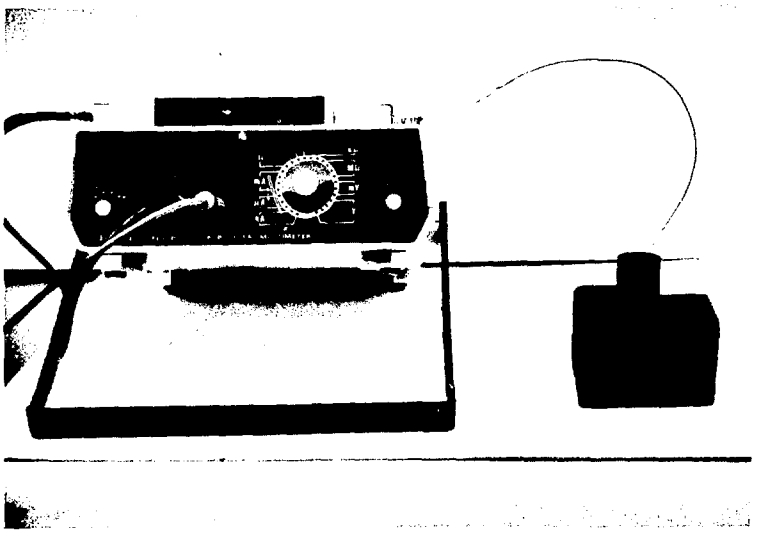

Fig. IV-1.
Measurement of the surface temperature of LWRHU.

E. Vibration

Representatives of LASL, Jet Propulsion Laboratory (JPL), NASA-AMES, FI, and APL met to review preliminary vibration test results for the LWRHU and to review the basis for the environmental specification that had been provided by JPL.

The random vibration environment is dominated by the response predicted for the interior of the Galileo probe. Most of the energy of the random environment comes from frequencies less than 400 Hz, which is the portion of the power spectral density envelope controlled by the Probe environment. NASA-AMES, GE, and Hughes Aircraft have formed a team to reevaluate the predicted environment within the Probe.

The sine environment is dominated by an antenna on the Orbiter at low frequencies (below 100 Hz). As currently specified the low frequency portion of the sine environment shows double amplitudes that are beyond the capability of test equipment.

At LASL an experimental search for resonant frequencies in a LWRHU fueled with simulant and insulated with PG found no indication of "impacts" or "chatter" with excitation up to levels of 5 G^2/Hz over the range of 10 to 2000 Hz when the excitation was perpendicular to the cylindrical axis of the unit. However, the excitation coincident with the cylindrical axis "chatter" was observed over the range of 10-150 Hz at input of 2 G^2/Hz and from 10-250 Hz with 3 G^2/Hz input. An increase in input raises the "intensity" of the chatter and extends the frequency upward. No unique resonant frequencies were observed.

F. Design Review

A design review of the LWRHU was held on 26 February 1980 at LASL with about 20 representatives from other interested organizations present. All aspects of the development of the LWRHU design were presented. The two most significant design problems yet to be adequately resolved are: 1) the APL's calculation of the marginal thermal response (possible melting of the clad) during the most severe reentry environment if only PG is used and 2) the inadequate vibration resistance of CBCF-3 (a better thermal insulator than PG) in the very severe launch vibration environment postulated and specified by the JPL and NASA-AMES. Calculations and vibration testing of several PG/CBCF composite configurations are in progress to resolve this dilemna.

V. FUEL PROCESSING

A. Processing

One lot of SRP feed powder (0.26 kg) was processed at LASL. The lot was O-exchanged and then ball-milled for 40 h and slugged and screened to form <125-μm granules. The granules were thermally seasoned and set aside for the fabrication of GPHS pellets.

B. Characterization

Analytical data for 2 containers of SRP feed powder enriched at 83.5 at.% ^{238}Pu are listed in Table V-1. The containers are SR Lot 440, Run 906923 (LASL Lot 38) and SR Lot 440, Run 906922 (LASL Lot 39). These lots were used to fabricate RHU production pellet lots RU 3 through RU 7.

Isotopic data for LASL lot 38 are listed in Table V-2. Neutron emission data for lots 38 and 39 are listed in Table V-3, together with data for RHU

TABLE V-1

ANALYTICAL DATA FOR SR FEED LOTS
(83.5 at.% ^{238}Pu)

	ppm by weight[a]	
Element	Lot 38	Lot 39
^{241}Am	121	119
^{237}Np	207	191
^{232}Th	510	470
^{234}U	1980	2080
^{236}Pu	0.61	0.73

[a]Isotopic values as of 10/16/79.

TABLE V-2

ISOTOPIC DATA FOR FEED LOT 39
(83.5 at.% ^{238}Pu)

Isotope	Wt%
^{238}Pu	83.49
^{239}Pu	13.95
^{240}Pu	1.97
^{241}Pu	0.46
^{242}Pu	0.13

pellet RU 3-1 made from feed lot 38. Spectrochemical data for lots 38 and 39, together with data for RHU pellet RU 3-5, made from lot 38, are presented in Table V-4.

C. Residues and Shipments

Approval has been received to ship the material for Residue Declaration RS-238-62 (1.0 kg ^{238}Pu). An additional 1.67 kg of plutonium oxide-containing residues (1.15 kg $^{238}P7$) has been packaged for shipment.

Five casks of SR feed enriched at 80 at.% ^{238}Pu and 3 casks of feed enriched at 83.5 at.% ^{238}Pu were received in February. In addition, one 62.5-W size GPHS pellet, made at SRL, was received. This pellet will be encapsulated in IR-0.3 W and impacted.

TABLE V-3

NEUTRON EMISSION DATA FOR SR FEED
(83.5 at.% ^{238}Pu)

Conditioned	Emission Rate (n/s-g ^{238}Pu) Lot 38	Lot 39	RHU Pellet[a] RU3-1
As Received	18 068	18 475	
^{16}O-Exchanged	13 558	9 156	
Seasoned Granules			
at 1100°C		7 716	
at 1600°C		6 765	
Sintered Pellet			5255

[a]RHU pellet RU3-1 fabricated using feed lot 38.

TABLE V-4

SPECTROCHEMICAL DATA FOR FEED
ENRICHED AT 83.5 at.% ^{238}Pu
(ppm by weight)

Species	Lot 38	Lot 39	RHU Pellet[a] RU3-5
Al	85	70	250
Ba	15	10	
Be	< 1	< 1	< 1
Ca	130	130	110
Cd	< 10	< 10	< 10
Co	3	5	5
Cr	70	130	45
Cu	15	15	5
Fe	240	300	280
Hf	< 25	< 25	< 25
K	8	3	< 5
Li	< 1	< 1	< 1
Mn	10	10	15
Mo	5	10	3
Na	2	3	2
Ni	45	75	30
Pb	15	5	5
Si	210	120	290
Sn	5	5	7
Sr	10	10	15
Ti	5	5	5
V	< 3	< 3	< 3
W	< 10	< 10	< 10
Zn	20	15	10
Zr	< 100	< 100	< 100

[a]RHU pellet RU3-5 was fabricated from feed lot 38.